DEVELOPMENT OF A HEIGHT CONTROL SYSTEM USING A DYNAMIC POWDER SPLITTER FOR DIRECTED ENERGY DEPOSITION (DED) ADDITIVE MANUFACTURING

By

VIVIAN ZHOU

THESIS

Submitted in partial satisfaction of the requirements for the degree of

MASTER OF SCIENCE

in

Mechanical and Aerospace Engineering

in the

OFFICE OF GRADUATE STUDIES

of the

UNIVERSITY OF CALIFORNIA

DAVIS

Approved:

Masakazu Soshi, Chair

Xinfan Lin

Stavros G. Vougioukas

Committee in Charge

2021

ABSTRACT

The directed energy deposition (DED) process is an additive manufacturing (AM) operation in which highly concentrated energy and metal powder/wire are applied onto a surface to general a metal clad. In this study, experiments were conducted utilizing blown powder DED in which the powder and laser are coaxial to each other in the nozzle housing. Utilizing computer numerical control (CNC), the powder and laser can be moved during the deposition process to generate a continuous clad to create metal objects ranging in geometric complexity.

Clad geometry is a function of laser energy flux, powder flux, laser and powder spot diameter, and energy (or temperature) state of the substrate. The working distance between the nozzle and the substrate can fluctuate throughout a deposition which will affect the powder flux and result in changes in the height of the clad. This is due to heat accumulation over time in the deposition piece. The constant laser power results in clads flattening from the heat, leading to the underbuilding of the part. These errors in height may compound over several layers within a deposition. While less evident in short builds, in longer and/or complex builds, the process can become so unstable that the part fails to build any longer.

The purpose of developing a height control system that uses a dynamic powder splitter was to manipulate the powder flux to maintain a designated working distance throughout an entire deposition. Monitoring of the working distance was achieved by a camera sensor, changes in powder flow rate (PFR) was achieved by a Dynamic Powder Splitting System (DPSS), and communication between devices was maintained by a microcontroller. Proportional integrative (PI) and proportional integrative derivative (PID) control systems were developed to correct the working distance errors during deposition, and they were compared to finalize the best control to be used in the overall system developed.

Thin wall depositions were conducted to analyze the controller's ability to correct layer-wise height errors. A comparison of the depositions in which the controller was active and inactive showed that each control system could control layer height effectively, resulting in more accurate part geometries. Ultimately, the PID control system created performed better by achieving higher stability and more accurate height control. Due to the development of this control system, more efficient and stable builds can be achieved which will greatly aid in a variety of additive manufacturing applications.

TABLE OF CONTENTS

LIST OF FIGURES

ACKNOWLEDGMENTS

I would like to express my profound appreciation and gratitude to Professor Masakazu Soshi for his support, guidance, and continuous encouragement throughout both my undergraduate and graduate career. Without him, I would not have been able to complete this project as it is today. His consistent dedication has inspired me to look past the many obstacles I have faced during this research process, and his optimism and passion for his work have influenced me to work my hardest—achieving goals I never thought I could accomplish.

I would also to like to show appreciation for the members of my thesis committee who have been patient with me throughout this process and my many setbacks due to COVID 19. They have continued to support me, and their efforts in reviewing my thesis have been invaluable. They are professors that I have and will continue to look up to long after I have left UC Davis. Their passion for their interests is what drew me to take on their courses and eventually reach out to them to become part of my committee.

I would like to thank DMG Mori for their generous support of the Advanced Research for Manufacturing Systems (ARMS) Laboratory. Their assistance was the catalyst for this research topic.

I would also like to thank the members of the ARMS lab that have supported me throughout my research. Kyle Odum, without your initial support, I would not have been able to even start my project. Your vast knowledge of additive manufacturing and mechanical engineering in general has always inspired me to reach greater goals. Thank you, Weijun Zhang, for your encouragement and help throughout my experiments. Your optimism has no bounds and has definitely influenced me to not always be discouraged. Last but not least, thank you to Curtis Yau and Nicholas Magnasco for not only being amazing lab mates, but amazing friends too.

Both of your constant reassurance throughout my graduate degree program is what really got me through this entire process. There have been many tough challenges, but also incredible memories and knowledge gained from this entire process. I would not trade it for the world, and I am excited for what the rest of my future holds.

1. INTRODUCTION

1.1. Background

As our technological progress continues to grow in complexity, the need for quick and efficient rapid prototyping grows as well. To iterate through several designs or visualize the manufacturing processes for mass production, one would use rapid prototyping to achieve quickly fabricated parts. This is commonly accomplished through additive manufacturing techniques.

1.1.1. Additive Manufacturing

Additive Manufacturing is a subsect of manufacturing where an automated process can create 3-D objects through layer-based fabrication. There are several methods being used to achieve additive manufacturing.

One such method is laminated object manufacturing (LOM) which consists of cuttings and laminating sheets of a material. Cut with a mechanical cutter or laser, the sheets are then bonded together. This is one of the first commercially available additive manufacturing methods available, and it is also able to be used for a variety of materials (polymers, ceramics, and metals) [1]. It is a relatively low-cost process that is used primarily for larger structures, but the disadvantages include bad surface quality and dimensional accuracy. This manufacturing method is also unable to create complex shapes.

Powder bed fusion is one type of additive manufacturing which consists of applying a laser beam or binder to fine powder that is spread across a platform [1]. This manufacturing method is the one most similar to the one that will be discussed in this paper. The advantages of powder bed fusion are the fine resolution and high quality of the final printed part which allows for complex pieces to be made, but there are drawbacks in using this method. The process itself is slow and

expensive, and when using a liquid binder, there will be high porosity in the part when the powder is fused together [1].

In this study, we will be focusing on Directed Energy Deposition (DED) as the additive manufacturing process.

1.1.2. Directed Energy Deposition (DED) Process

The Directed Energy Deposition Process is achieved through applying highly concentrated energy to metal powder/wire onto a surface to generate a metal clad. While there are several types of energy and feedstock available, this study is examining the DED process that utilizes a high-power laser and metal powder to generate the metal clad for building a metal part. This is different from powder bed fusion because there is no powder bed; instead, there is a powder stream that is fed coaxially with the laser. The process can achieve complex parts with great mechanical properties and controlled microstructure, but disadvantages include low accuracy and surface quality in the final part [1]. It is commonly used in the automotive and aerospace industry. An example of which can be seen below in Figure 1.1.

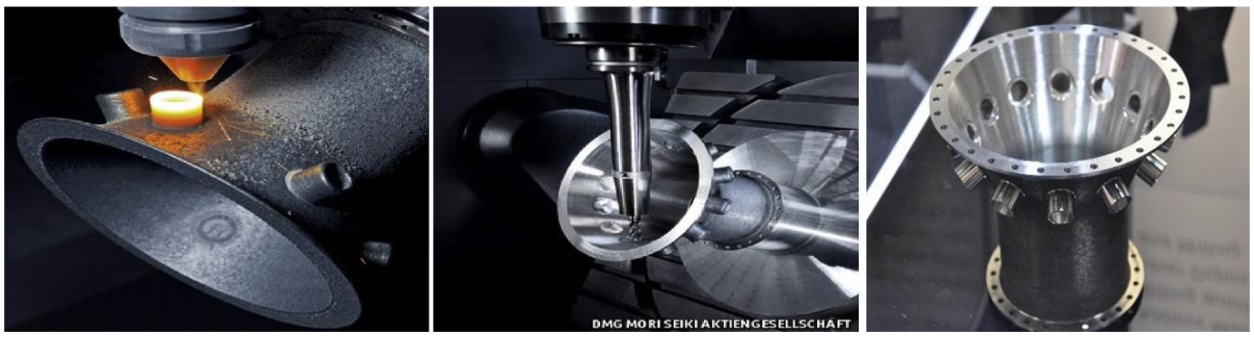

Fig. 1.1: Turbine housing that was created through the DED process. (Left) The part created through multi-axis deposition. (Middle) The part being machined for a better surface finish (Right) The final finished turbine [2].

1.1.3. Limitations of DED and Current Approaches

There are areas in which DED can be improved upon. The DED process is characterized by low accuracy due to instabilities as a result of heat accumulation and working distance changes due to a variable melt pool shape. During long builds, heat accumulates in the part, which causes the clad width to increase while the clad cross-sectional area remains constant, leading to a shorter clad. The flattening of the clads can cause both part underbuilding and severe sloping at the ends of thin wall parts [3]. This typically results in underbuilding during the process, as can be seen by Figure 1.2, where the working distance is higher than normal, and the actual height is lower than ideal. In order to combat this, passive and active working distance control is utilized. The working distance of the nozzle to the substrate affects the powder flux into the meltpool [4], which affects clad height [5].

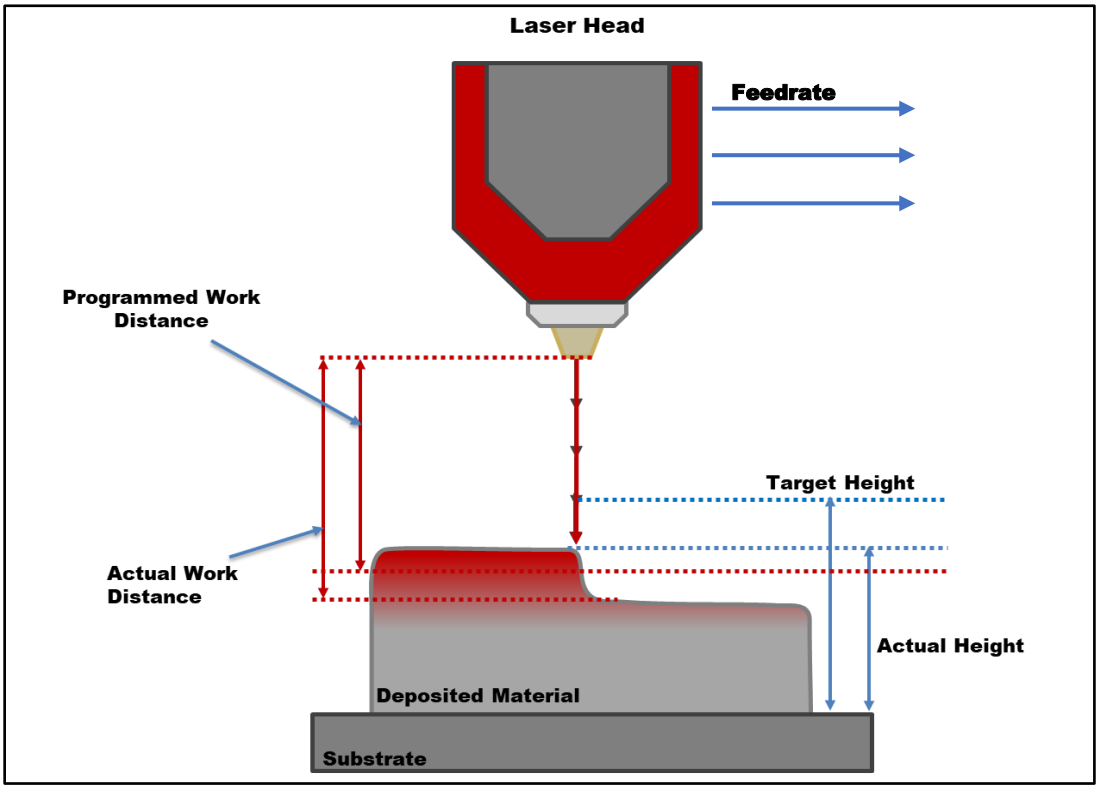

Fig. 1.2: Common Directed Energy Deposition Error

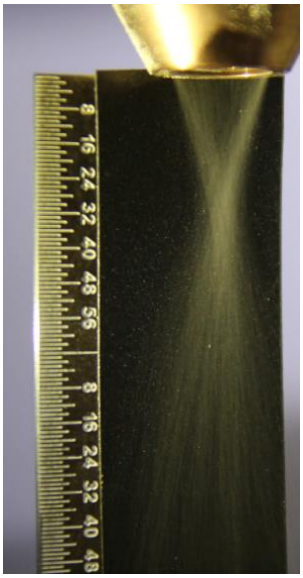

Fig. 1.3: Image of the powder cone from the LaserTec 65D

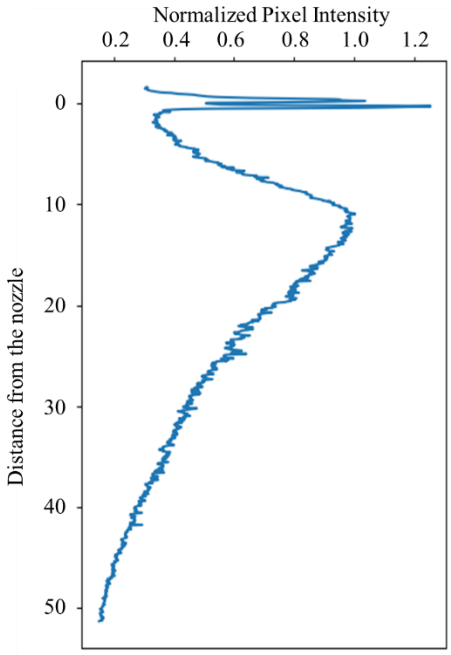

Fig. 1.4: Normalized pixel density curve of the powder cone in Figure 1.3

Passive working distance control is unique to the geometry of the powder cone in the DED process [6]. Visualized in Figure 1.3, the powder cone has its pixel intensity extracted from the image to illustrate a curve that gives an idea of the actual powder density distribution, seen in Figure 1.4. The hollow powder cone is achieved by the convergent nozzle within the machine directing the powder towards a common point, the meltpool. DED clad height has been shown to be directly proportional to the PFR into the meltpool [5]. The commonly used working distance is 11mm from the nozzle which is just before the maximum powder concentration point in the powder cone. This allows for corrections for both under- and overbuilding during the DED process. If the part is overbuilt for a layer, the working distance decreases, resulting in a lower powder density that creates a shorter clad in the proceeding layer, ideally correcting the height error. Conversely, if the part is being underbuilt, the working distance increases, resulting in a

higher powder density that creates a taller clad in the proceeding layer. However, as seen in Figure 1.4, there is only a small portion the passive working distance control is able to correct underbuilt parts. Additionally, this passive correction is slow and is effective in correcting small variations in layer height. As height error propagates through the layers in the DED process, the underbuilding can become so severe that the meltpool descends past the maximum powder concentration, resulting in the process becoming so unstable that deposition ceases completely [7].

Active working distance control methods have been developed and studied, but techniques developed that are able to correct the errors must interfere with the NC code, alter the powder flow rate (PFR), change machine feedrate, and/or adjust laser power during deposition. The drawback of modifying the NC code during the deposition process is that this would have to be done periodically, causing the cycle time to increase [8, 9, 10]. Adjusting the powder flow rate typically results in a slow time response which is not effective in correcting real-time errors [11, 12]. The relationship between feedrate and clad height requires complex calculation and values to be obtained through extensive experimentation which is costly and time-consuming, and simulations used to facilitate obtaining these values require adaptive programming which can become complicated to develop [13]. While it is simple to adjust the laser power, the parameters used to calculate the adjustment value are difficult to extract during the deposition process as well requiring complex simulation [14].

1.2. Literature Review for Active Control Methods in DED

Many studies have been conducted to develop active control systems that are able to both measure the working distance or clad height during the DED process and adjust parameters to compensate

for the errors identified during deposition. There are advantages and disadvantages to each of these methods which will be explored within this section.

1.2.1. Clad Height Measurement Techniques

There is currently no tool or device within the machine that is able to record and measure the height of the workpiece during deposition. A study was conducted in which a touch probe was used to measure the workpiece [8]. While incredibly accurate at a standard uncertainty value of 2.1×10^{-4} mm, the probe device could not work in conjunction with the deposition process as it needed to replace the laser head in the machine via the automatic tool changer. Due to this, the cycle time significantly increased, and measurement was not conducted for every layer.

Garmendia et al., in [9] and [10] use a light scanner to obtain a height profile of the deposited layer in the DED process. This device is fixtured externally within the machine so that it will not inhibit the deposition process. By projecting light onto the piece, a measurement can be obtained in the form of a three-dimensional point cloud as long as the field of view contains the top of the piece. An example of this may be viewed in Figure 1.5, where the point cloud is plotted in MATLAB to show a range of depth measurements across the top of the cladded piece.

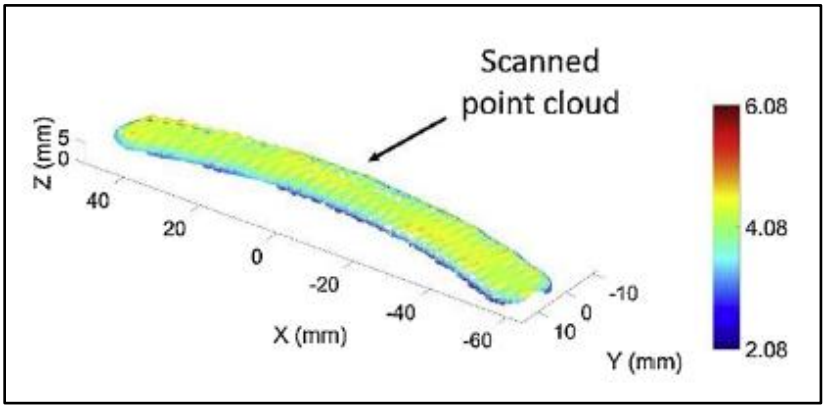

Fig. 1.5: Height profile of a layer created by the light scanner [9]

There are some drawbacks to this setup. The precision of the measurement is entirely dependent on the calibration of the equipment, but with correct calibration, a 0.05mm precision can be obtained. An initial scan of the base is needed to create a coordinate system to translate and rotate the scan due to the fact that the light scanner is attached away from the laser head and adjusted to angle towards the part. This calibration process also needs to be performed prior to deposition which increases the manufacturing time, but due to being a relatively simple process, it does not affect the time by much. This measurement process also requires that the deposition process be stopped, so this method is not done every layer for this study.

A laser scanner or laser displacement sensor has also been used for measurement [11]. With a measurement range of ±40mm and a resolution of 8 μm, this device is highly accurate and can be applied for a variety of deposition heights. The main drawback listed in this study is that the height profile measurement required a significant amount of time. While the specific response time was not listed, the convergence time of the algorithm that utilized this sensor ranged from 4 to 10 seconds, depending on the layer. This was greatly improved when incorporating an iterative learning control (ILC), decreasing convergence time to roughly 0.05 seconds. However, this required a complex setup, experimentation, and simulation to produce.

Cameras have been used in a variety of ways to measure the height during the DED process as well. In Song et al. [14], a triangulation setup is created with three CCD cameras. All three cameras are used to measure the height of the piece, and the results are compared against each other to increase the robustness of the system's decision making, shown in Figure 1.6. The triangulation setup requires some information to be known and measure beforehand such as the distance from the camera to the piece, focal length of the camera lens, and the angle of the camera which all can affect the accuracy of the measurement.

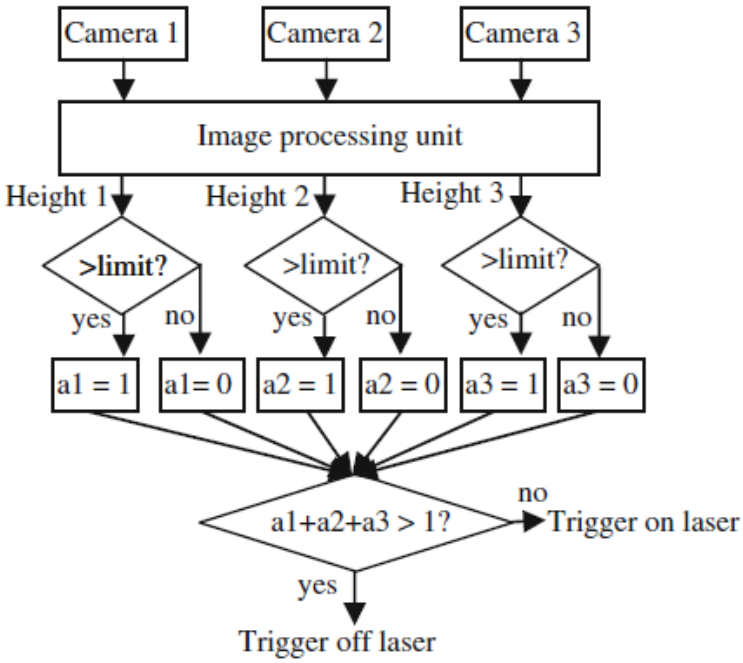

Fig. 1.6: Logic Diagram of the height measurement system that incorporates three cameras to triangulate the height.

Zeinali et al. [13] studies the use of a single CCD camera which is calibrated using an image of an object where the size is known. Some image analysis and filtering are required to produce a viable measurement, but this seems to be typical for most of the camera systems that have been developed for DED-related purposes [12, 13, 14].

Another single camera system is studied with a different configuration. The camera is integrated within the laser head along with a line laser that is attached externally to the laser head. When the line beam is shone onto the cladded piece, the shift in the beam can be used to calculate a measured height. This is best visualized in Figure 1.7. Equations are used to calculate the height based on the camera's pixel size, projection angle of the line beam, and the transverse magnification of the imaging system. When compared against a conventional high accuracy height

measurement tool, this system touts an accuracy of ±50-μm when measuring the final height of the experiment pieces.

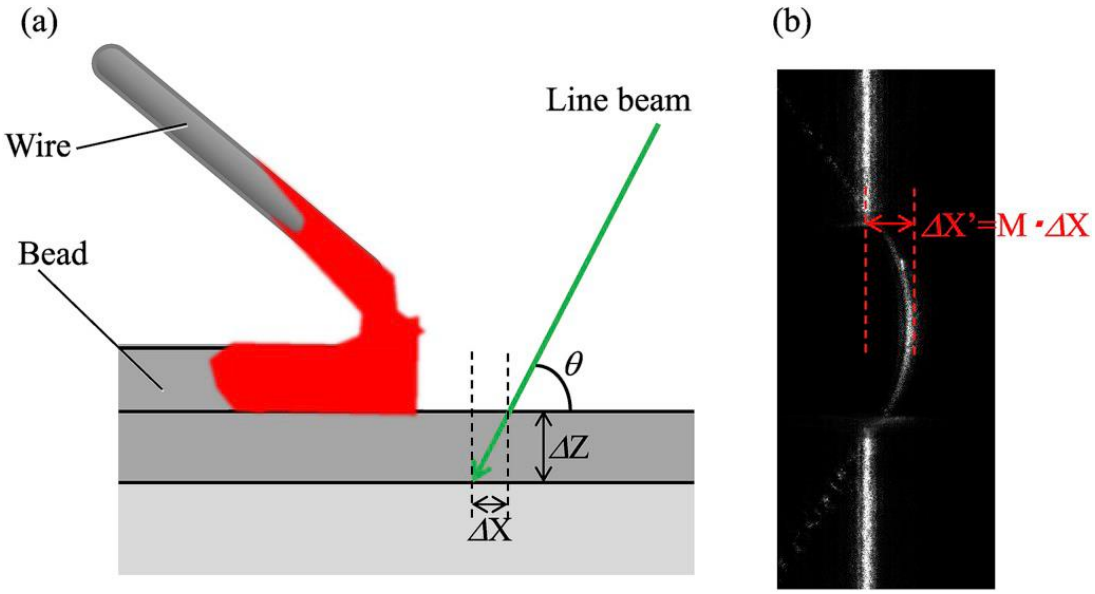

Fig. 1.7: (a) Line beam and camera measurement system with (b) an example image of the line beam captured by the imaging system [12].

1.2.2. DED Parameter Control for Height Correction

Various process parameters can affect the clad height in the directed energy deposition process. As can be seen in Figure 1.8, laser powder, powder feed rate, carrier gas flow rate, and stand-off distance all can manipulate the resulting clad height [15]. Therefore, some research pertaining to maintaining an ideal clad height during the deposition process concerns controlling either one or a combination of these parameters.

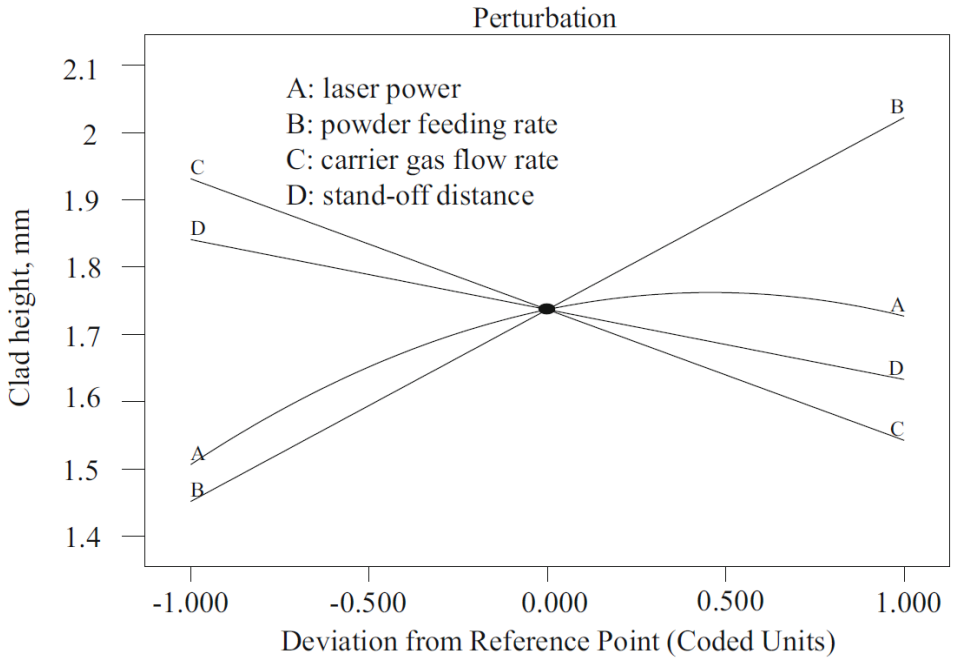

Fig. 1.8: Graph illustrating how various DED parameters affect final clad height [15].

Laser power modulation is simple to perform and has been found to be quite efficient in maintaining deposition height in one study [14]. However, in order to distinguish the appropriate laser power to correct deposition height errors, both clad height and meltpool temperature were required. This increases the complexity and cost of the overall system as a hybrid controller is needed in order to couple the sensor inputs.

NC code adjustment requires active comparison between the programmed height and the actual part height and period modification of the NC code [8, 9, 10]. By determining the height discrepancy during deposition, the NC code is modified to add or remove layers depending on whether the part is under- or overbuilt, respectively. Studies conducted using this method end up increasing the cycle time due to having the change the program. To combat this, the measurement of the piece and adjustment of NC code are not done continuously and instead, performed in layer intervals which is not ideal.

A study was conducted in which adjusting the velocity of the substrate (feedrate) was utilized to correct deposition height errors [13]. However, the parameters needed to calculate an effective output feedrate are extremely sensitive to variation, and the DED process is quite dynamic. Extensive experimentation would be needed to identify model parameters. This study produced an adaptive sliding mode controller that would be able to account for uncertainties in the parameters, unmodeled dynamics, and external disturbances. The control system developed became quite complex in order to preserve stabilities and robustness.

PFR modulation is effective at controlling clad height while not affecting the build quality or microstructure of the deposited material [11]. However, due to the slow time response of most PFR control systems in DED machine tools, implementation requires complex model-based controllers to handle the time lag between powder feeder mechanism commands and changes of PFR at the deposition nozzle. Takushima et al. [12] was able to circumvent this issue due to the fact that their experiments used wire-fed DED. Changing the wire-feeding speed is a lot quicker due to the feeding mechanism being closer to the nozzle. A dynamic power splitting system (DPSS) was created for powder DED that is able to adjust PFR quicker (from several seconds to less than half a second) by being incorporated into the machine at a point closer to the deposition nozzle [16].

1.3. Scope of Research

1.3.1. Motivation

One of the motivations behind this research is resolving the inconsistencies in clad height during the DED process. Since height errors propagate through layers, process stability requires a consistent nozzle working distance to ensure that the height of the layer is ideal. While there is

research being performed to examine how to fix these inconsistencies in the deposition process, current techniques involve changing the laser power, PFR, feedrate, or adding/removing layers in the deposition which can end up increasing the cycle time, cost, and complexity of the system as well as require changes to the original programming of the machine. All of which are undesirable. Therefore, another motivation of this research is to not only resolve these errors but be able to do so without increasing undesirable factors that can impede on the use of the DED process. By determining a method that can measure the height and alleviate the deposition errors without increasing cost and cycle time, this lesser used manufacturing process can also be utilized more within industry to fix or create complex parts with cheaper cost.

1.3.2. Research Objective

The current height compensation approaches require additional changes to the NC programming or complex monitoring of the system to achieve ideal working distance during the deposition process. These approaches to compensate the deposition errors lengthen the manufacturing process time and at times does not completely resolve the target height errors. The goal is to develop a control system to dynamically control the powder flow during the DED process to correct the errors in clad height. By creating a system that can rapidly adjust the PFR without modifying the NC program, a more accurate part can be created without forfeiting manufacturing time or additional materials.

1.4. Research Approach

1.4.1. Overview

The system that was developed to solve the issues forementioned is essentially a three-part system—two of which were developed in this paper, and one was developed previously [16]. The input to this system is the clad height error or working distance error during deposition. This is achieved through a measurement system that includes a camera sensor that is able to record and analyze the meltpool's location during the DED process. The output would be a change in the PFR, achieved through the Dynamic Powder Splitting System (DPSS). The DPSS is a previously developed hardware that has significantly improved the DED process by allowing PFR adjustment to be achieved within half a second. This will be integrated into the machine via the third part of the system: the controller. The controller is a program that is able to take in the input from the camera, translate the information, and control the DPSS to produce a respective output. This program is connected to the DPSS through a microcontroller (an Arduino). The system components that are within the machine itself are shown below in Figure 1.9. The controller program and Arduino are not depicted as they are managed outside of the LaserTec.

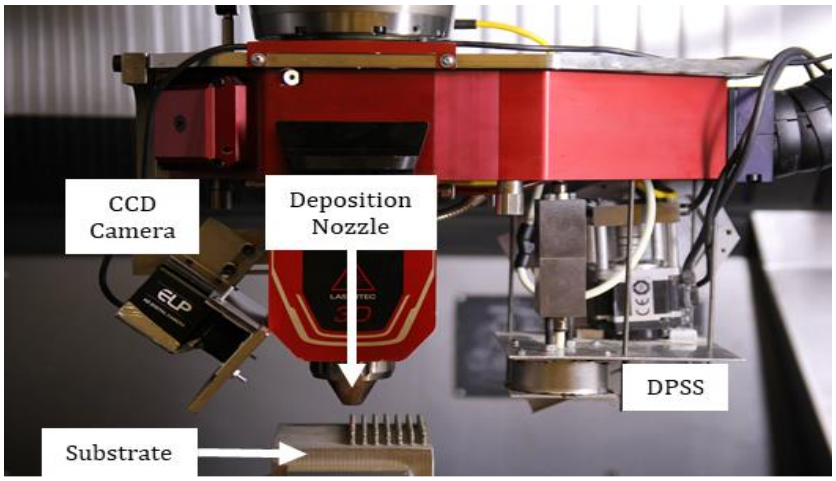

Fig. 1.9: Height controller system within the LaserTec 65 3D.

1.4.2. Elements of the Control System Design

Powder flow rate was controlled and tested using two versions of control. The first iteration of the system used proportional integrative (PI) control, and the second version used proportional integrative derivative (PID) control. Both functioned based off of inputs established by the observed deviation of the nozzle working distance from the target working distance. Based on the linear relationship between clad height and PFR into the meltpool, the calculated working distance error is translated into a new PFR that is used to ascertain a new DPSS powder splitter position. A microcontroller is used to send signals from the controller to the DPSS to adjust the PFR during deposition.

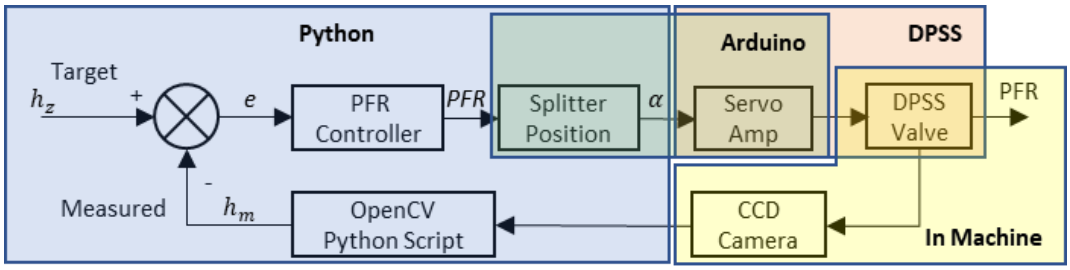

Fig. 1.10: Height Controller Block Diagram

Figure 1.10 illustrates how the individual components of the height controller work in conjunction with each other. Using input from the camera, the Python program communicated with the DPSS via the Arduino to adjust the PFR during deposition.

1.4.3. Benefits of the Control System

By changing the PFR during deposition, it is now possible to maintain the shape accuracy of the deposition piece without changing the path programming, laser power, or number of layers in the

DED process. Conventional methods need updating the NC code, feedrate, or laser power which can increase the manufacturing time, process complexity, and production costs. By having a controller that can dynamically and rapidly change the PFR between layers, the deposition time is preserved, and the geometry of the part can be improved.

2. CONTROL SYSTEM DESIGN

2.1. Optical Nozzle Working Distance Monitoring

Optical monitoring of the working distance is accomplished using a charge-coupled device (CCD) camera mounted on the deposition head behind a shade 11 welding glass. The welding glass allows for the camera to be able to view the meltpool by darkening the lens. The camera sends greyscale images at 25 Hz to a python script running on a computer external to the DED machine. Meltpool pixels are located using a global threshold binarization followed by an 8-way connected-component function from the OpenCV computer vision library. The nozzle working distance is calculated as the distance from the topmost pixel in the meltpool to the known location of the nozzle in the frame. The camera resolution is 960 pixels and operates typically around 8.8 pixels/mm.

This measurement system is able to achieve real-time feedback for the control system which is an advantage over many measurement systems being used in research for this manufacturing process currently. Many implementations require the DED process be paused to perform measurements or require complex calculations which causes a lag in the information being sent to a controller. By having the camera feed continuously active within the control program, the controller is able to receive visual data with little to no lag and perform analysis quickly so that the DED process can perform within a standard manufacturing cycle. The disadvantages of this

approach, however, include being less accurate than other measurement methods such as with a laser or touch probe. Due to the resolution of the camera, the camera is able to analyze about 0.11mm (translated from 1 pixel) of change, but this can be improved upon by swapping for higher quality/resolution cameras. Additionally, since the camera sensor is installed within the machine, this attachment obstructs some of the movement of the machine; while it is not a critical detriment for common build operations, it is worth noting.

2.1.1. Optics Background

Due to the angle in which the camera is positioned respective to the nozzle and substrate, measurement from the center of the meltpool in the frame is not accurate. This can best be visualized in Figure 2.1. Therefore, the measurement will be taken from the top of the meltpool as that is assumed to be the top of the clad during deposition.

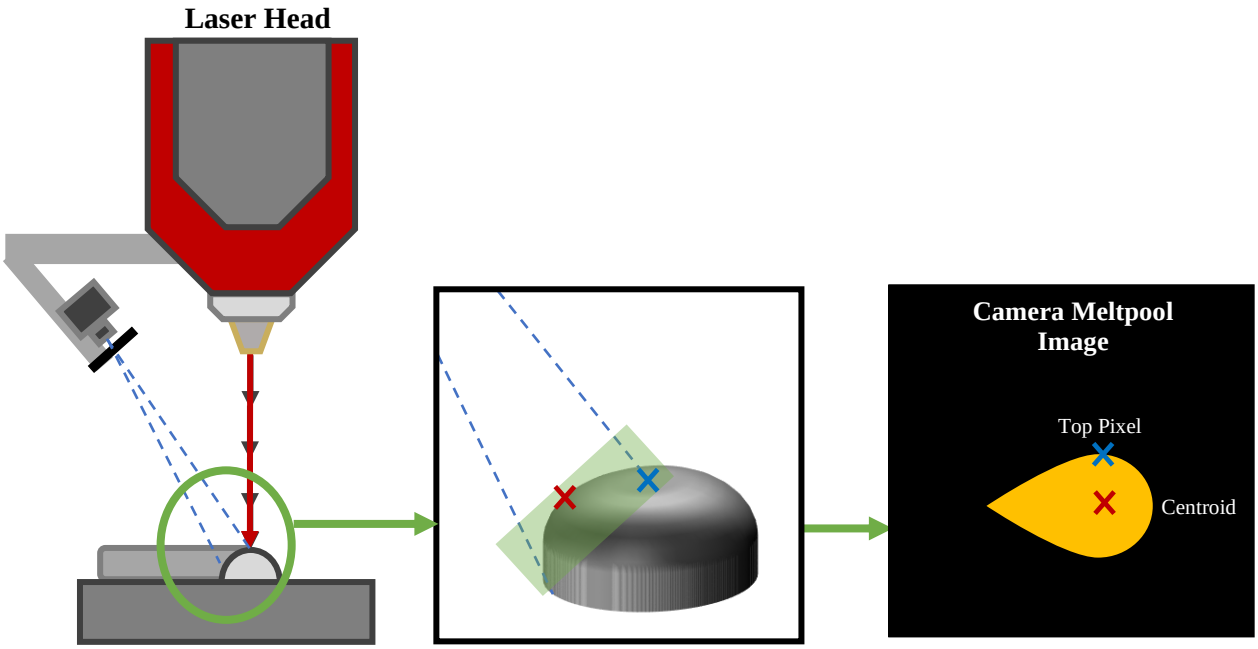

Fig. 2.1: 3D geometry of the clad/meltpool is viewed by the camera.

Initial tests were performed assuming that the centroid of the meltpool during DED was the top of the clad for measurement. However, when compared against calipers, there was a common discrepancy discovered between all the tests using this point in the frame as a measurement reference. Re-calculating the measured clad heights by using the same DED footage but with a height analysis concerning the top of the meltpool, measured heights that were centered around the ideal height was found. Thus, all experiments shown in this paper are performed by identifying the top pixel of the meltpool during deposition for measurement purposes.

2.1.2. Calibration Methods

To measure the working distance from this top pixel, a relationship between the pixels within the camera frame and the actual physical distance must be established. This is achieved by using a stepper block to determine this assumed linear relationship.

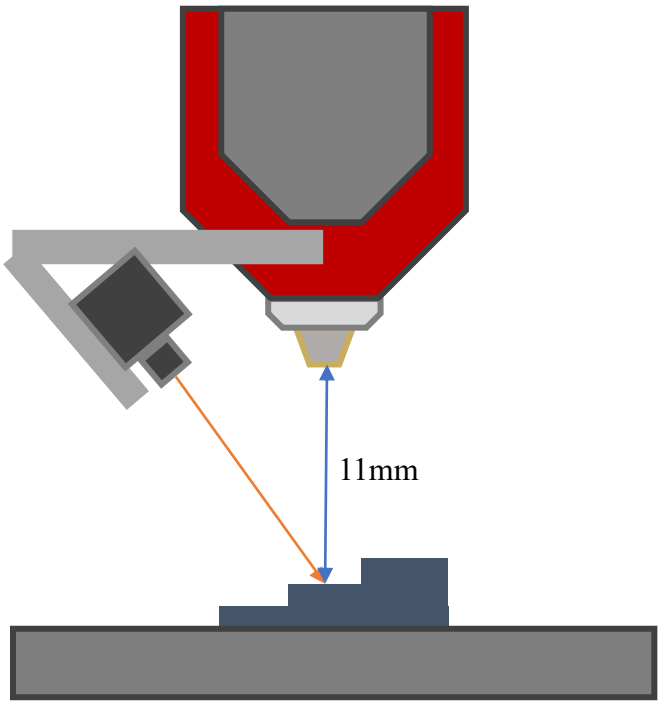

Fig. 2.2: Calibration Technique with Stepper Block

A pilot laser is used in the calibration process. It is a non-invasive light shone through the nozzle of the machine which mimics the position of the laser. Using the pilot laser-driven onto a metal block, a mock meltpool is generated to analyze the pixel data, as seen in Figure 2.2. With camera sensors, there is the possibility of a fisheye effect that can skew the image. An exaggerated example of this can be seen in Figure 2.3. There are potential calibration methods in order to circumvent the distortion for accurate measurement, but this would require additional precise measurements of the lens radius and center and complex setup to obtain the degree of spherical distortion [17].

Though a linear relationship between pixels and physical distance is established, this fisheye distortion would skew this ratio, complicating image analysis. However, under the assumption that deposition errors should not vary largely (within 1mm), by positioning the camera so that the pilot laser is centered within the frame, we avoid much of the fisheye effect. A stepper block with three steps at heights 10mm, 11mm, and 12mm is used to ascertain the pixel-to-mm ratio.

Fig. 2.3: Fisheye effect in cameras [17]

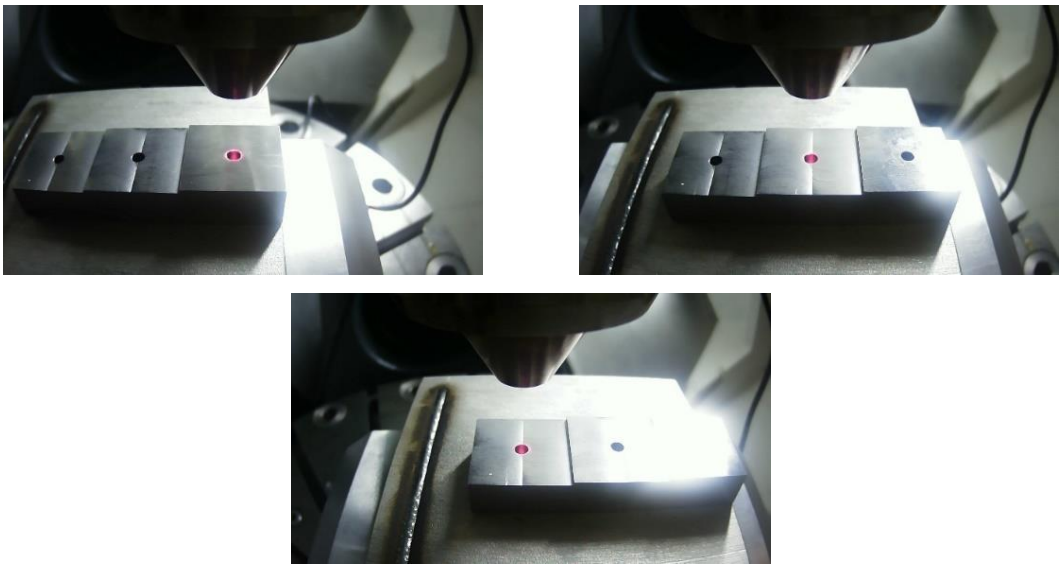

Fig. 2.4: Calibration Stepper Block Photos at Different Steps

To begin the calibration process, the nozzle is first positioned 11mm above the middle step which is the ideal working distance during deposition. Then, by taking the centroid pixel position of that spot in the frame, we can use it as a reference point. The steps to the left and right of it have a 1mm height difference, so by shining the pilot light over these steps, we simulate the placement of the meltpool when the process is under- or overbuilding by 1mm. By finding the pixel difference in the positioning of the light when compared to the middle step, we get the pixel-to-mm conversion value, Pm.

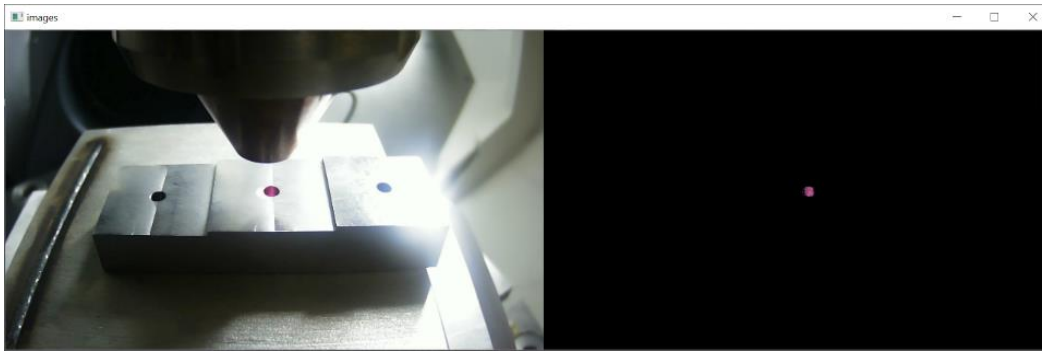

Fig. 2.5: Calibration Stepper Block with Laser Point Extracted

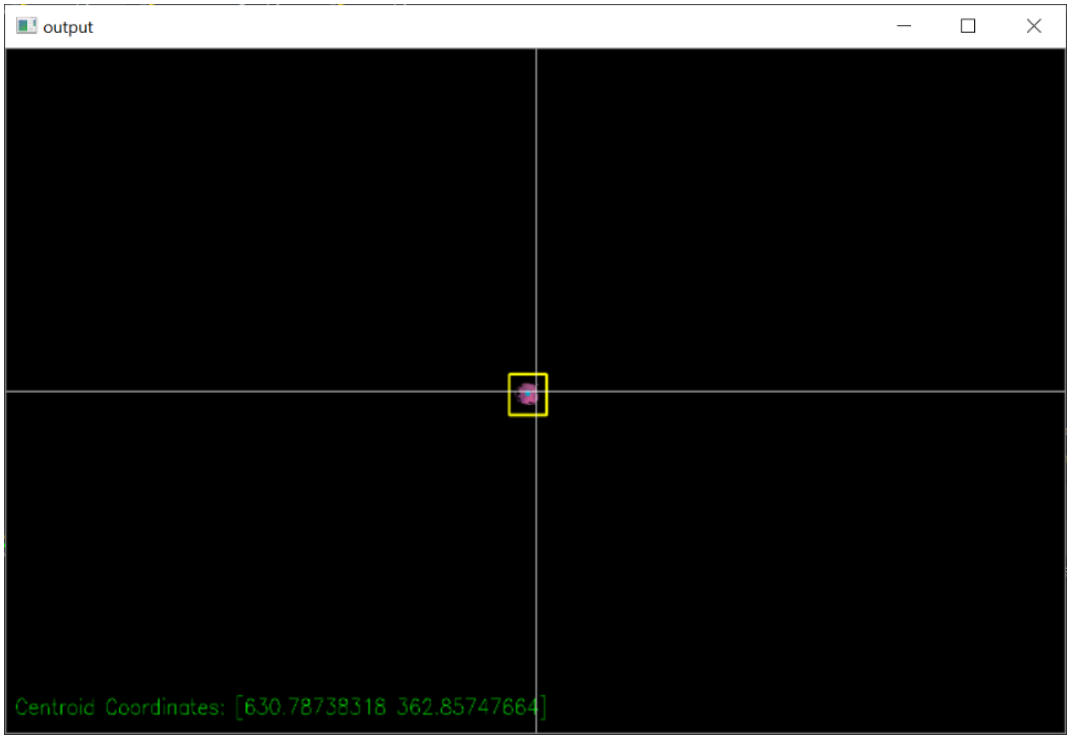

Fig. 2.6: Extract Laser Point Pixel Centroid Coordinates

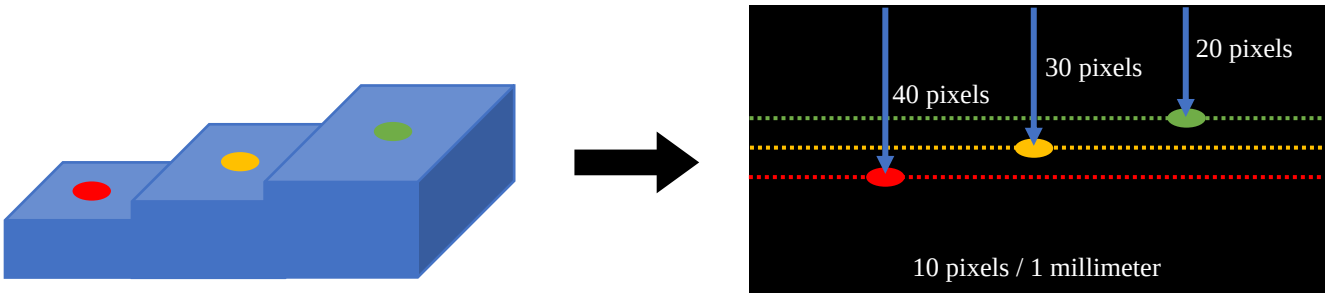

Fig. 2.7: Visual showing how the pixel-to-mm ratio is calculated from the various images from the stepper block.

To maintain the working distance, an ideal pixel y-axis location must be located. Preliminary tests concluded that using the pilot laser 11mm away from the substrate does not give an accurate position. However, by performing a laser raster operation, an ideal meltpool position in the frame can be obtained. A laser raster is simply a back-and-forth tool path in which the laser is on, but

there is no powder flow. Since no material is deposited, the process does not build. However, the laser still creates a meltpool on the surface of the substrate. Using the centroid pixel for this process gives an appropriate estimate for the ideal working distance.

With an ideal y-axis to maintain the meltpool and a ratio to convert pixel distance into physical millimeters distance, a working distance error or clad height error can be calculated for the deposition process.

2.1.3. Measurement Technique

As mentioned above, the calibration process prior to deposition establishes a y-axis line within the frame, where z = 0. Using Equation 1, the working distance error of the deposition process can be obtained.

$$\boldsymbol{E_{wd}} = h_z \; - \; (h_b - h_c) \cdot Pm \tag{1}$$

The y-axis in which z = 0 is set at the y-position in the frame, h_b. The top of the clad is h_c. The difference between the base and the top of the clad is used to determine the height of the clad in pixels which is then multiplied by the pixel-to-mm ratio, Pm. The measured height of the clad is subtracted from the ideal height of the clad, h_z, to calculate the working distance error.

Due to the nature of the process, the clad height can also be calculated from the working distance equation, as seen in Equation 2. The relationship between these two equations can best be visualized in Figure 2.8. The image shows how if the part is underbuilt, the error in working distance and the error in clad height are the same value, just with different sign values. A part that is shorter increases the working distance as the base upon which the next layer is build is farther

away from the nozzle. Similarly, this means that the clad piece is shorter by that same error amount, indicating a negative error.

$$\mathbf{e} = -E_{wd} = (h_b - h_c)Pm\ - h_z \tag{2}$$

The ideal clad height, h_z, is determined based on the retract of the nozzle between each layer. The pixel-to-mm conversion value, Pm, is established during the calibration process. The last two height or y-distance values are obtained through analyzing each frame the camera records during the deposition process.

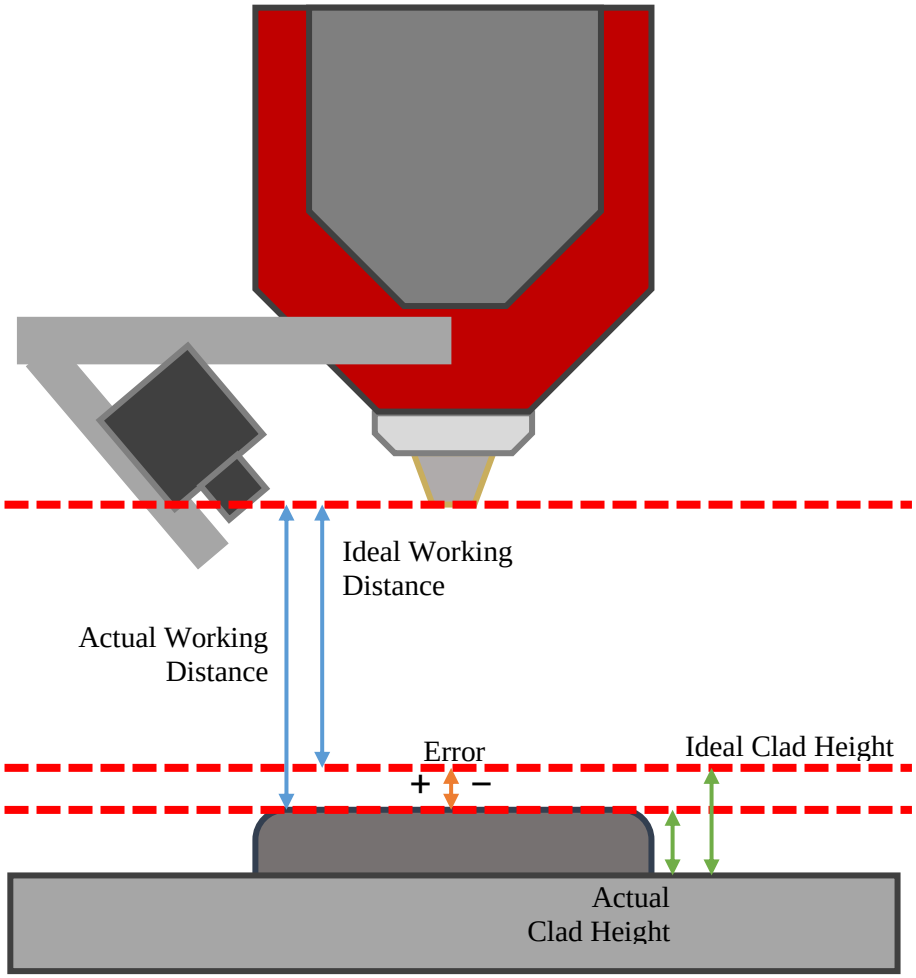

Fig. 2.8: Relationship between the error in working distance and error in clad height.

By analyzing the top of the meltpool during deposition, we can calculate any discrepancies from the desired working distance. An example to better understand this measurement process is included in Figure 2.9. For this example, if the desired clad height for every layer in a deposition is 1mm and the pixel-to-mm ratio is 15 pixels/mm and the top pixel of the meltpool is 5 pixels lower than expected, then the part is underbuilding by 0.3mm. That error is then used in calculating a desired PFR to alleviate the error for the next deposition pass. The calculations are demonstrated in Figure 2.10.

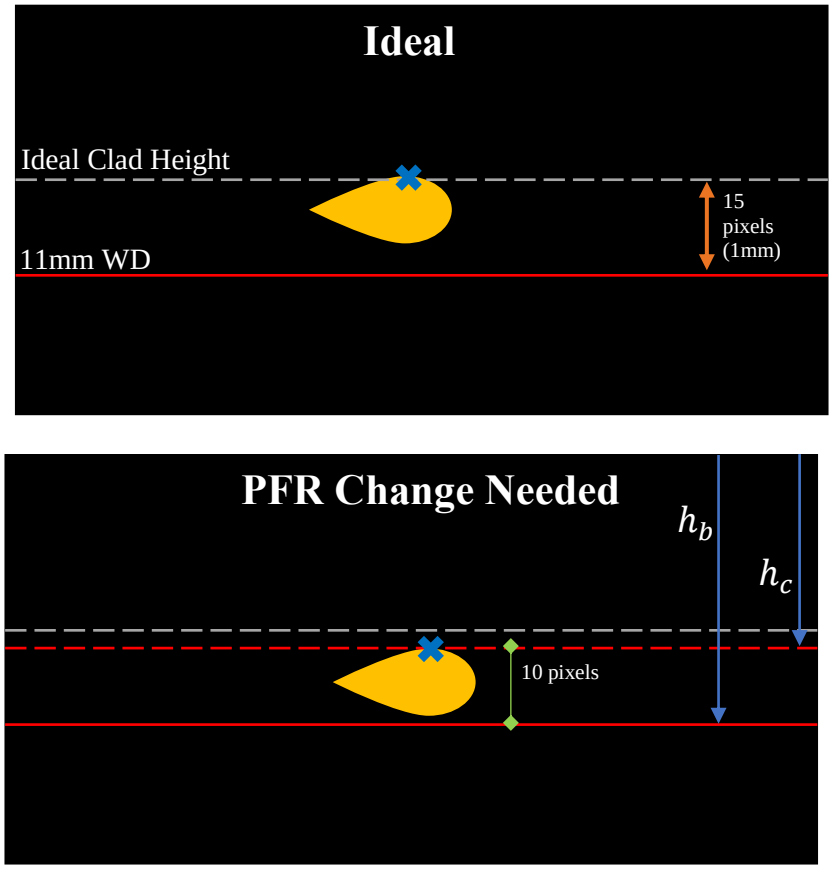

Fig. 2.9: Example of the meltpool analysis for height measurement

$$(h_b - h_c) = 10 \text{ pixels}$$

$$\boldsymbol{E_{wd}} = h_z - (h_b - h_c)Pm = 1\text{mm} - (10\text{px})\left(\frac{1}{15}\frac{\text{mm}}{\text{px}}\right) = 0.3\text{mm}$$

$$\mathbf{e} = -E_{wd} = -0.3\text{mm}$$

Fig. 2.10: Calculations for clad height measurement based on the example in Figure 2.9.

The working distance error is found to be 0.3mm, indicating the working distance is 11.3mm. Thus, it can also be concluded that the clad height error is -0.3mm, indicating the clad height is roughly 0.7mm instead of 1mm. This discrepancy would be adjusted by changing the PFR as the next step in the control system.

2.1.4. Camera Fixture Design and Implementation

To attach the camera sensor to the LaserTec 65, six individual components were designed and fabricated to create a prototype fixture, as shown in Figure 2.11. Working drawings were created and sent to DMG Mori for machining.

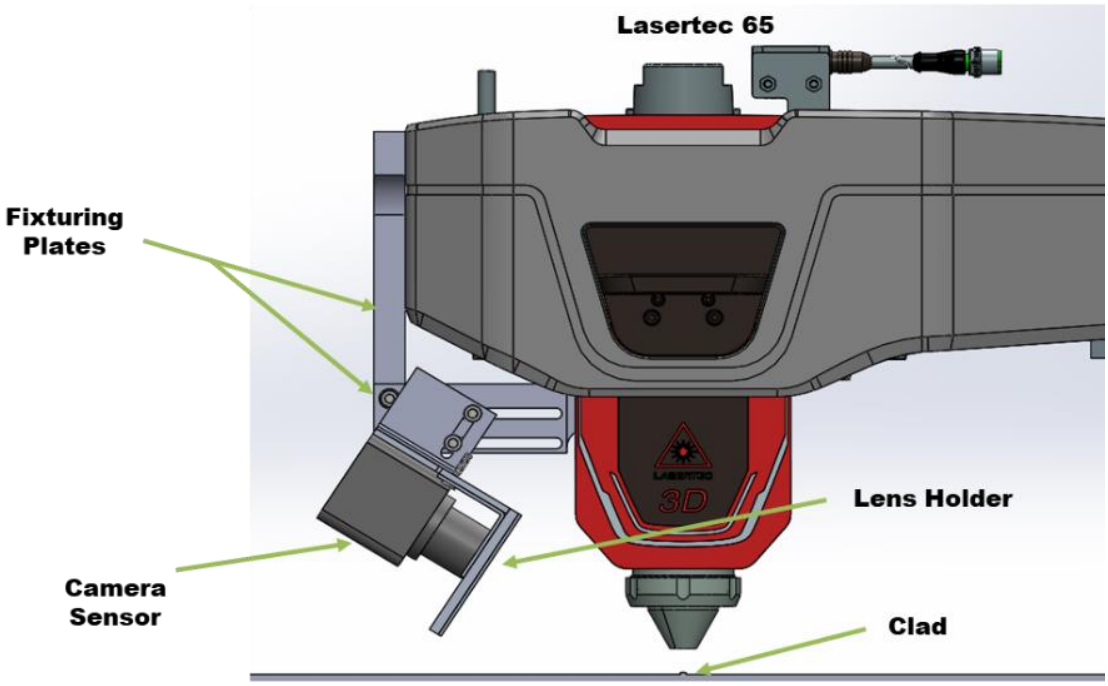

Fig. 2.11: CAD Screenshot of the Camera Fixture Assembly

The design of this fixture needed to be rigid in order to prevent the camera from jostling during the deposition process. Since the nozzle will be moving, any jostling of the camera would skew my input and make analysis basically impossible. Therefore, two fixturing plates were designed to minimize movement along the X and Y axes. One plate attaches on to the machine on the left side and one attaches to the back of the nozzle housing. Slots for the bolted connections were created for tolerancing.

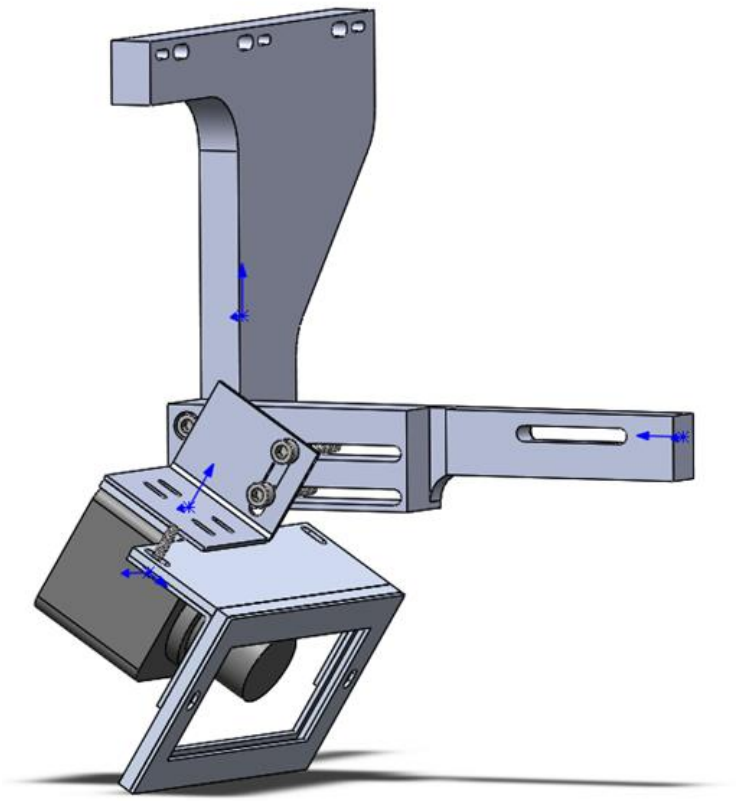

Fig. 2.12: All the mechanical fixture components used to attach the camera system to the existing machine.

In order for the camera to be able to view the deposition, a welding lens was used to darken the lens of the camera enough to be able to see the meltpool. A picture frame design was used as a holder for the lens. This would attach to a T-Shaped piece via L-Brackets found on McMaster. The lens holder components are shown in Figure 2.13.

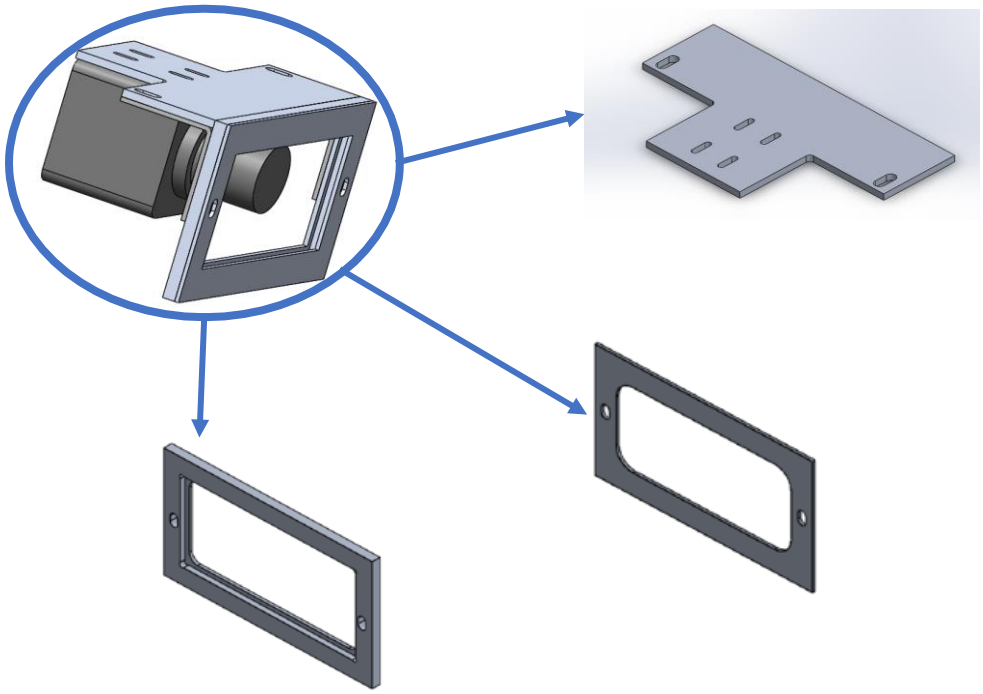

Fig. 2.13 Lens holder components.

To connect the camera to the plates on the machine, a simple sheet metal attachment plate was designed that would bolt onto the camera and one of the fixture plates, Figure 2.14. Without knowing the ideal distance and angle to place the camera within the machine, this piece had to be able to be adjusted laterally and be rotated, but also fixed into place. A two-slot design was implemented, the functionality of which is shown in Figure 2.15.

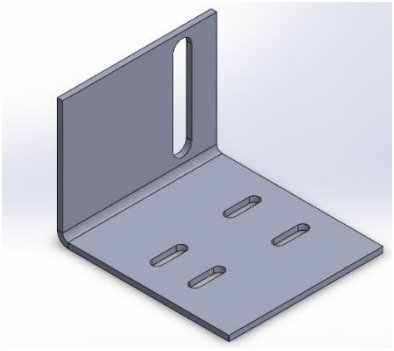

Fig. 2.14: Camera attachment plate.

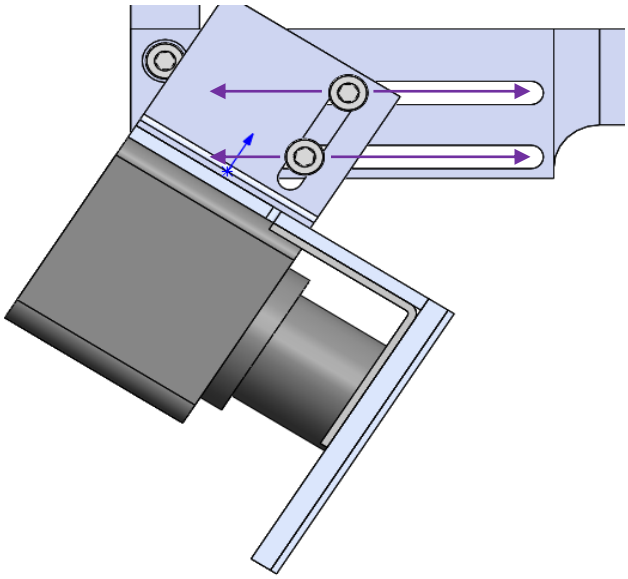

Fig. 2.15: Two-slot design allowing for lateral movement and rotation of the camera.

An FEA on the plate itself was conducted to ensure that the thickness of the sheet metal would keep the camera rigid, shown in Figure 2.16. By estimating a weight for all the fixture components and the camera itself, a 2.9N downward force was translated over the entire plate portion of the plate. Split lines were used to imitate two 10mm washers that would be used to bolt the bracket. After analyzing the maximum deflection angle that would occur, the design was deemed sufficient for experiments.

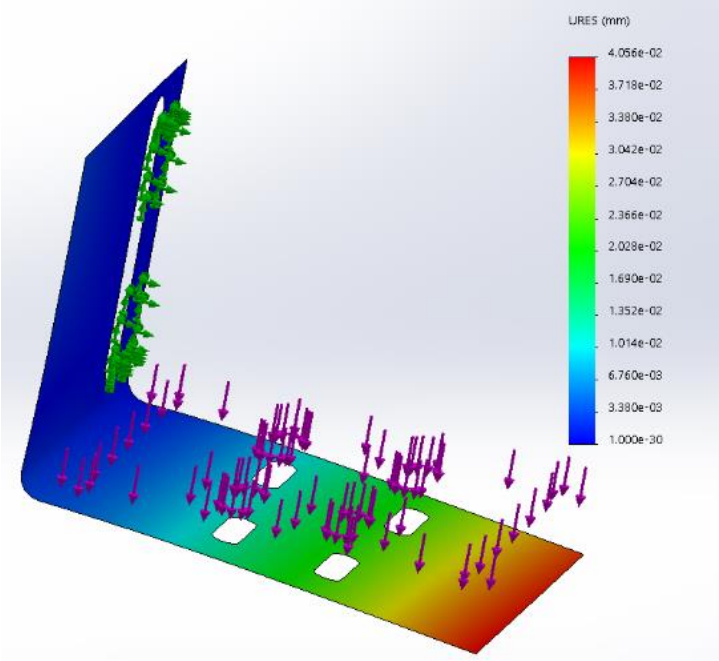

Fig. 2.16: FEA of the camera attachment plate, showing deflection based on the estimated load of the camera and its attached components.

2.2. Dynamic Powder Splitting System

2.2.1. System Function

The Dynamic Powder Splitting System (DPSS) is a complementary system to the main powder feeding system used within the DED process [16]. This system allows for rapid PFR modulation due to its placement near the nozzle of the system. The main powder feeding system in the machine is connected roughly 3m away from the cladding system, which leads to a time response of several seconds when changing the PFR during deposition. Utilizing the DPSS, the time response is lowered to less than half a second.

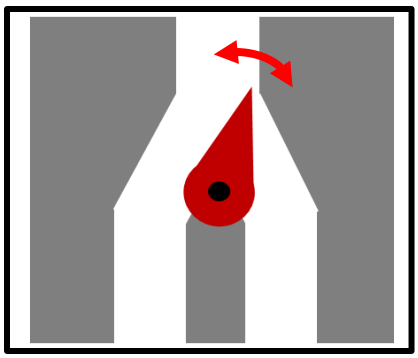

Fig. 2.17: Valve Design

2.2.2. Components of the System

This system consists of a custom valve actuated by a servomotor that can split the powder flow from the main powder feeding system and the inert gas stream that drives the powder to the nozzle. By splitting the powder flow, the powder flow rate can be changed right before being sent to the nozzle. Splitting the gas stream allows for the split powder (not going to the nozzle) to be recycled for further use in the deposition.

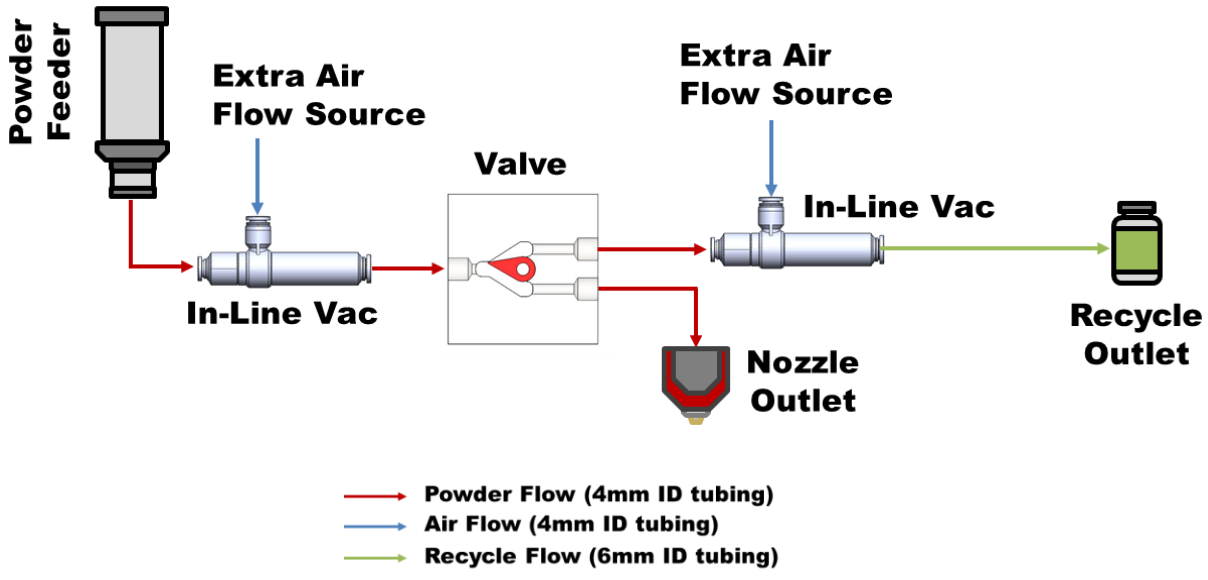

Fig. 2.18: Components of the DPSS System

In the figure above are the various pieces that make up the DPSS. The in-line vacuums are used for powder mixing and as a conveyance mechanism to move powder further along the tubing. The valve's full range of movement is around 22.4°. In order to ascertain the powder flow rate that is conveyed at certain powder positions, a calibration process is performed. The resolution of the powder splitter is 0.2 degrees for the experiments performed in this paper. The calibration process performed consisted of performing powder flow rate tests to determine the powder flow rate at various positions in the powder splitter (typically at angles 6, 8, 11.2, 14, and 16°). Then, a curve fit is performed, typically giving a curve like in Figure 2.19.

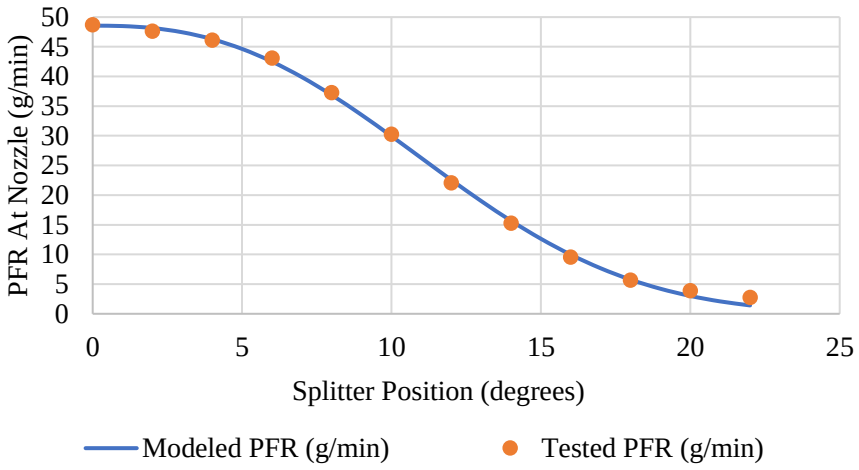

Fig. 2.19: Curve fit using Equation 3 for DPSS operating with PFR0 = 50 g/min.

$$PFR = PFR_0 \times A \times \mathrm{EXP}(-k \times \alpha^n) \tag{3}$$

A, k, and n are fitting constants determined from PFR tests. They are determined by finding the values for A, k, and n that produce the least sum of squared residuals based on Equation 3. The

adjusted equation to solve for the angle is Equation 4. This angle is sent to the Arduino from the Python program to begin the actuation of the motor in the DPSS. This can be viewed in Figure 2.20.

$$\alpha = -1/k \times [ln(PFR/(PFR_0 \times A))]^{\frac{1}{n}} \quad (4)$$

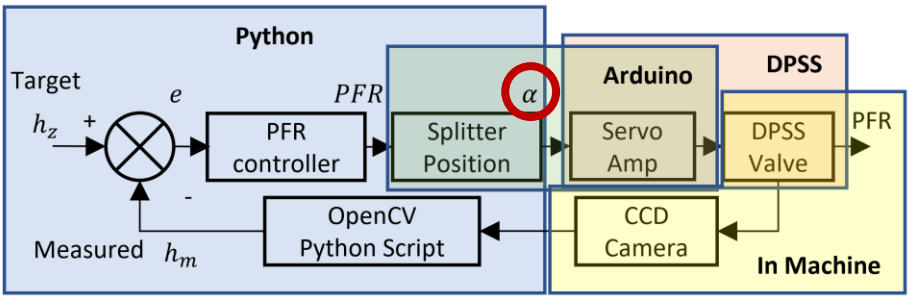

Fig. 2.20: The height controller block diagram with the powder splitter angle highlighted.

2.2.3. Benefits of the Dynamic Powder Splitting System

An important factor in the additive manufacturing process is reducing the operation time. In standard depositions, changing the PFR will require several seconds before the adjustment is complete. By utilizing the DPSS, the PFR response time can be reduced from several seconds to less than 0.5s [16]. This allows for more bandwidth in the time it takes the controller calculate the working distance as well as maintain consistent deposition procedures.

2.3. Controller Program

2.3.1. Height vs. Powder Flux Estimation

Based on previous empirical data, a linear proportional relationship was found between the clad height and the powder fluence during deposition, shown in Equation 5.

$$h_c = C \times PFR/(F \times d_l) \quad (5)$$

$$F = feedrate;\ d_l = laser\ spot\ diameter$$

This equation was adjusted to create a PI and PID controller to counteract errors determined by the camera sensor during deposition. By determining the corresponding increase or decrease in PFR to achieve a change in clad height, the following deposition pass should be able to offset the error from the previous layer.

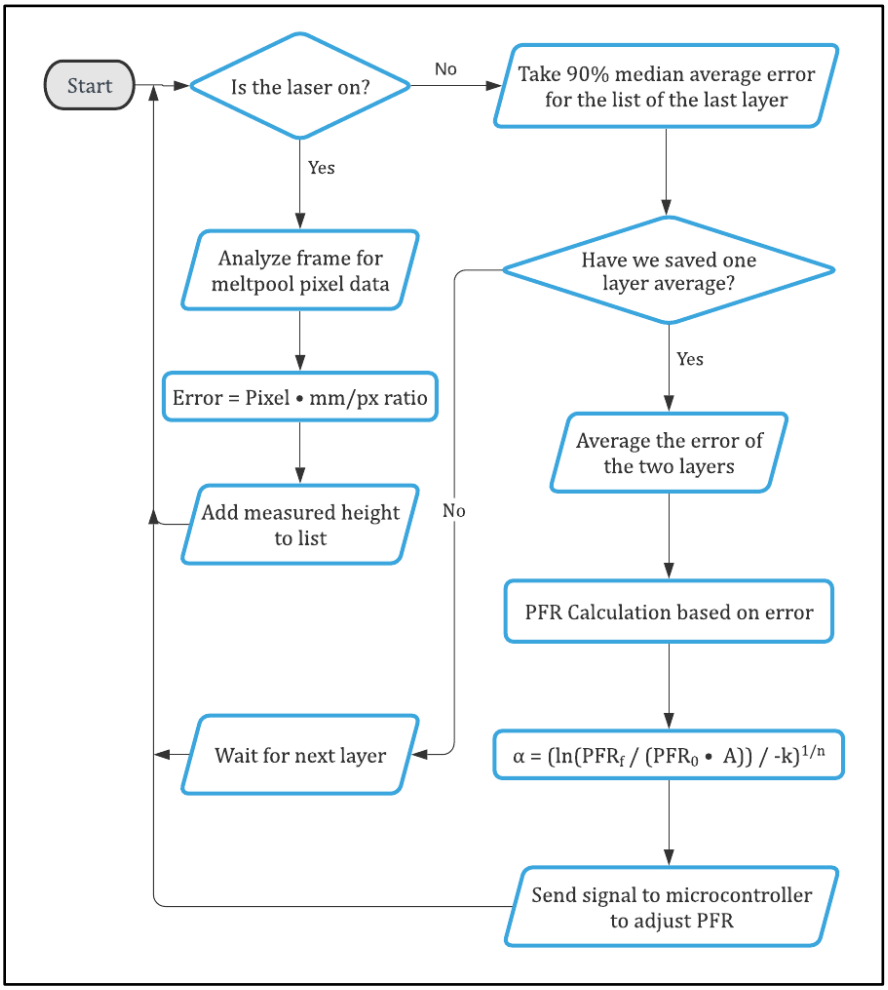

Fig. 2.21: Controller Logic Diagram

A diagram depicting the decision making of the overall control system is shown in Figure 2.21. The trigger to begin measurement recording is if the laser is on, and the meltpool is observed within the camera frame. The program begins analyzing the meltpool pixel data to determine the top pixel of the meltpool and translate it into a mm value to put into a list. Once the laser is determined to be off, indicating the layer is finished, the control system then checks if a layer-wise average has been saved previously. If not, the control system waits to have two lists of measurement values for two adjacent layers before beginning the correction analysis. A 90% median average is taken on the list of measurement values across a single later. This is to eliminate outliers and also counteract typical geometric trends in the deposition process. Typically, due to the nature of the process, the ends of the layer turn out to be sloped slightly higher than the middle. Once a 90% median average is determined and averaged with an adjacent layer's 90% median average, the final mm error is used in the PI or PID controller equation to determine a respective PFR to correct the error. This PFR uses Equation 4 to calculate the angle in the powder splitter to create the PFR for the next deposition pass. A signal is sent to the DPSS via the Arduino to actuate to this angle position.

Averages are performed every two layers due to the directionality of the laser in the y-axis during deposition. There are at times misalignments in the laser that cause the meltpool to be viewed as skewed during the deposition process. To combat this phenomenon without demanding extremely accurate laser positioning tuning, averages are performed. The directionality can be viewed in Figure 2.22.

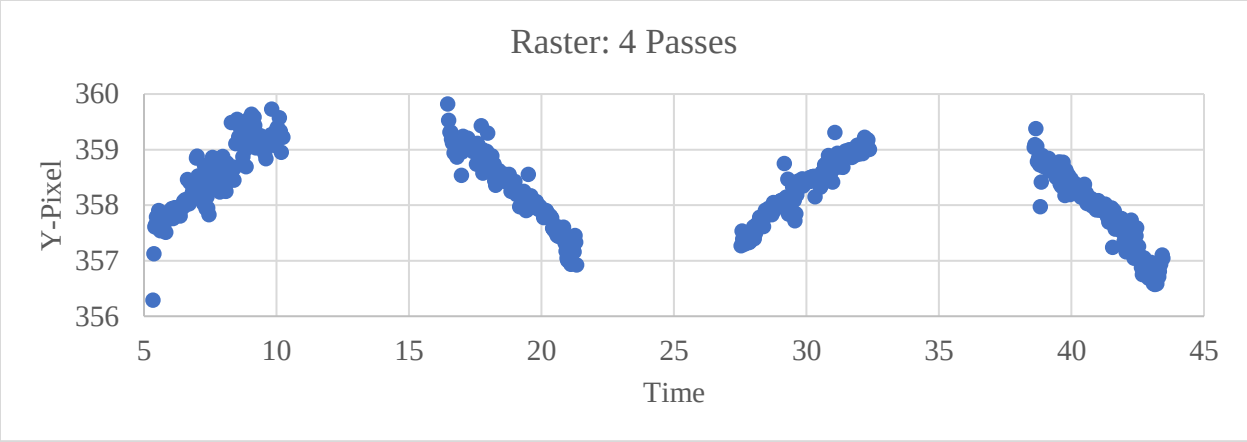

Fig. 2.22: Sample Raster Data

2.3.2. Proportional Integrative (PI) Control with Moving Averages

A PI controller was created using Equation 6 to compensate for the deposition errors.

$$PFR_{i+1} = PFR_i + (h_{wd} - h_{wd0})(F \times d_l)/C \tag{6}$$

Due to the laser not being perfectly aligned with the nozzle, there is some directionality to the measurement of the deposition. This is managed by taking moving averages across the layers recorded by the controller program. This is illustrated in Figure 2.23.

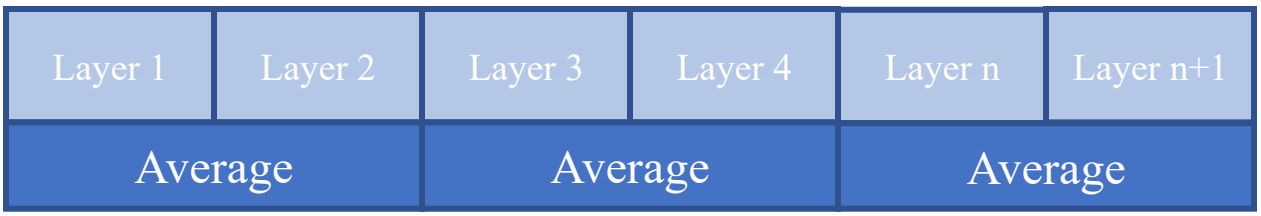

Fig. 2.23: Moving averages for the PI Controller

2.3.3. Proportional Integrative Derivative (PID) Controller Gain Tuning

After deposition experiments were tested with the PI controller, data indicated that the control system was susceptible to oscillatory behavior. The working distance fluctuated during longer depositions without stabilizing. To dampen this behavior and improve the time response of the system, Ziegler Nichols tuning was utilized to adjust the gain of the proportional, derivative, and integrative portions of the controller and identify the ideal gain values for our purposes.

Table 2.1: Effects of Increasing Individual Gains in PID System *[18] [19]*

Response	Rise Time	Overshoot	Settling Time	Steady-State Error	Stability
Kp	Decrease	Increase	Minor Increase	Decrease	Degrade
Ki	Decrease	Increase	Increase	Major Decrease	Degrade
Kd	Minor decrease	Decrease	Decrease	Minor Change	Improve

The Ziegler-Nichols method is a common PID tuning method that uses a systematic approach and pre-defined equations [20]. The first step is analyzing the system response as a P-controller, by reducing the integrative and derivative gains to 0. Changing the proportional gain until stable, steady oscillations occur in the response of the system results in finding the critical value where $K_p = K_{cr}$. The period of the sustained oscillations is also important, P_{cr}. Using these values, the equations for tuning are seen in Figure 2.24.

PID Type	K_p	T_i	T_d
P	$0.5\,K_{cr}$	∞	0
PI	$0.45\,K_{cr}$	$\frac{P_{cr}}{1.2}$	0
PID	$0.6\,K_{cr}$	$\frac{P_{cr}}{2}$	$\frac{P_{cr}}{8}$

Fig. 2.24: Ziegler-Nichols Gain Equations [20]

2.3.4. Proportional Integrative Derivative (PID) Control

The equation developed for the PID controller is seen below in Equation 7. From the gain tuning in the previous section, the sufficient gains determined are shown in Table 2.2.

$$PFR = (F \times d_l)[(K_p \cdot e) + (K_i \cdot \int e\, dL) + (K_d \cdot \frac{de}{dL})] \quad (7)$$

Table 2.2: Gains used for PID Controller Testing

Kp	Ki	Kd
0.6	0.2	0.45

Overlapping averages are used for this PID control as this was determined to improve errors in calculation from directionality. Figure 2.25 shows how this is achieved.

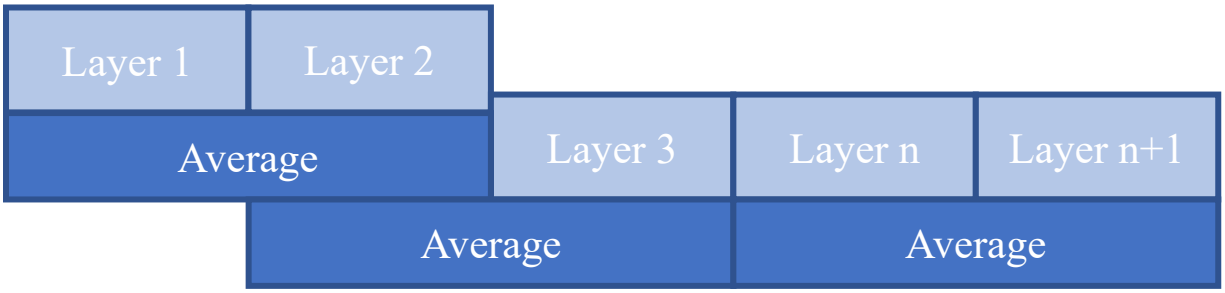

Fig. 2.25: Overlapping averages for the PID Controller

3. EXPERIMENT SETUP AND DESIGN

3.1. Thin Wall Depositions

3.1.1. Description

All deposition experiments were performed in an LT65 3D using gas atomized 316L stainless steel powder feedstock with particle sizes between 45 – 105 µm and argon as the shield and carrier gases. The 2.5 kW diode laser in the LT65 3D is focused to a circle with a radius of 1.514 mm through a Fraunhofer COAX9 deposition nozzle that has a nominal working distance of 11 mm to the base of the clad. DED and NC parameters included in Table 3.1 were kept constant over all tests conducted and presented in this paper.

Table 3.1. DED and NC parameters kept constant during testing

Parameter		Value	Unit
Feedrate		1	m/min
Carrier Gas Flow		6	l/min
Shield Gas Flow		6	l/min
Laser Power	Layer 1	1700	W
	Layer 2	1600	W
	Layer 3	1500	W
	Layer 4+	1400	W

Three sets of single-pass, thin wall deposition experiments were deposited with raster toolpaths to compare the performance of the height control system to DED without the controller. All thin walls were 80 mm long, approximately 3 mm wide, and were deposited onto hot rolled 316L bar stock substrates that had been milled flat.

3.1.2. Importance

Thin wall depositions are a simple process that is the building block for more complex depositions for DED. It is as it sounds, a basic back-and-forth movement of the laser and powder that creates a linear layer that builds upon itself. Depositions with several layers such as this become a thin wall type shape. This simplistic deposition style allowed for uncomplicated parameter changes to produce a variety of experiments. Its simple shape also allowed for simple measurement without having to complicate the deposition path due to the placement of the camera in relation to the nozzle (to avoid collisions).

3.2. Sensor and Actual Measurement Comparison

Experiments were performed to test the efficacy of the controller in managing deposition height errors. Comparison to an actual height, though, was needed to ascertain the accuracy of the camera sensor system. Using a Micro-vu measurement system, the height of each thin wall was measured to analyze how closely related the true height was to the final error determined by the controller.

3.3. PI vs PID Control Comparison

Initial testing utilized a PI controller, but further testing indicated that there are drawbacks. PI control tends to increase oscillatory behavior, which is undesirable during the deposition. Ideally, the controller maintains a stable PFR throughout the DED process. A PID controller was then implemented instead and tested for its efficacy in reducing the oscillations. The two controllers' results are compared to identify the best control system implementation for future work.

4. TESTING AND RESULTS

4.1. Thin Wall Experiments

4.1.1. 10-Layer Thin Wall with Constant Layer Height

Initial experiments to test the controller were performed using the parameters outlined in Section 3.1.1. An initial PFR of 23.5g/min was used, and previous testing showed that this produced a layer height of 0.83mm. A 5-second interlayer dwell time was used to allow for heat to diffuse during the deposition and allow for sufficient time for the controller to send commands to the DPSS. Five tests were performed with each controller and without the controller, totaling fifteen 10-layer depositions. Ten layers were chosen for these initial experiments to establish that the controllers implemented in parallel with the standard DED process do not adversely affect it. The final working distance error for all three deposition scenarios are compared in Figure 4.1.

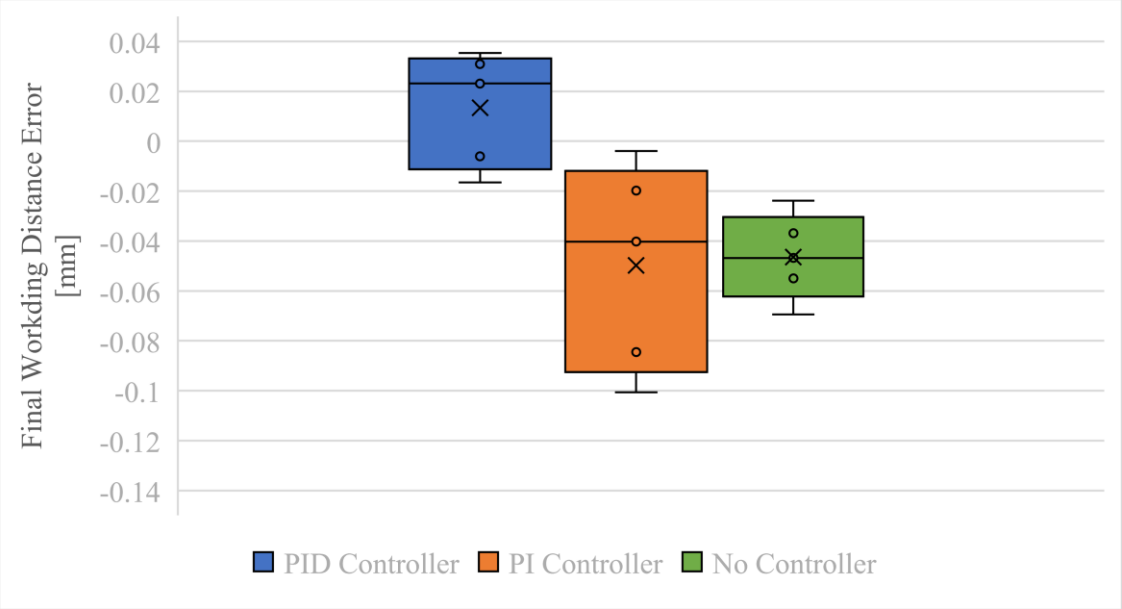

Fig. 4.1: Final part error from the 10-layer thin walls

4.1.2. 20-Layer Thin Wall with Nonconstant Layer Height

To demonstrate the ability of the height controller to quickly compensate for drastic underbuilding during DED, 20-layer thin walls were deposited with and without the controller using NC code with layer height errors deliberately included. Instead of a constant 0.83 mm layer height, the deposition nozzle was retracted 1.33 mm in Layers 5 through 7 (additional 0.5mm), totaling 1.5mm of working distance error introduced by the end of Layer 7. Both depositions were conducted with an initial PFR of 23.5 g/min and interlayer dwells of 5 s. The results can be viewed in Figures 4.2 and 4.3.

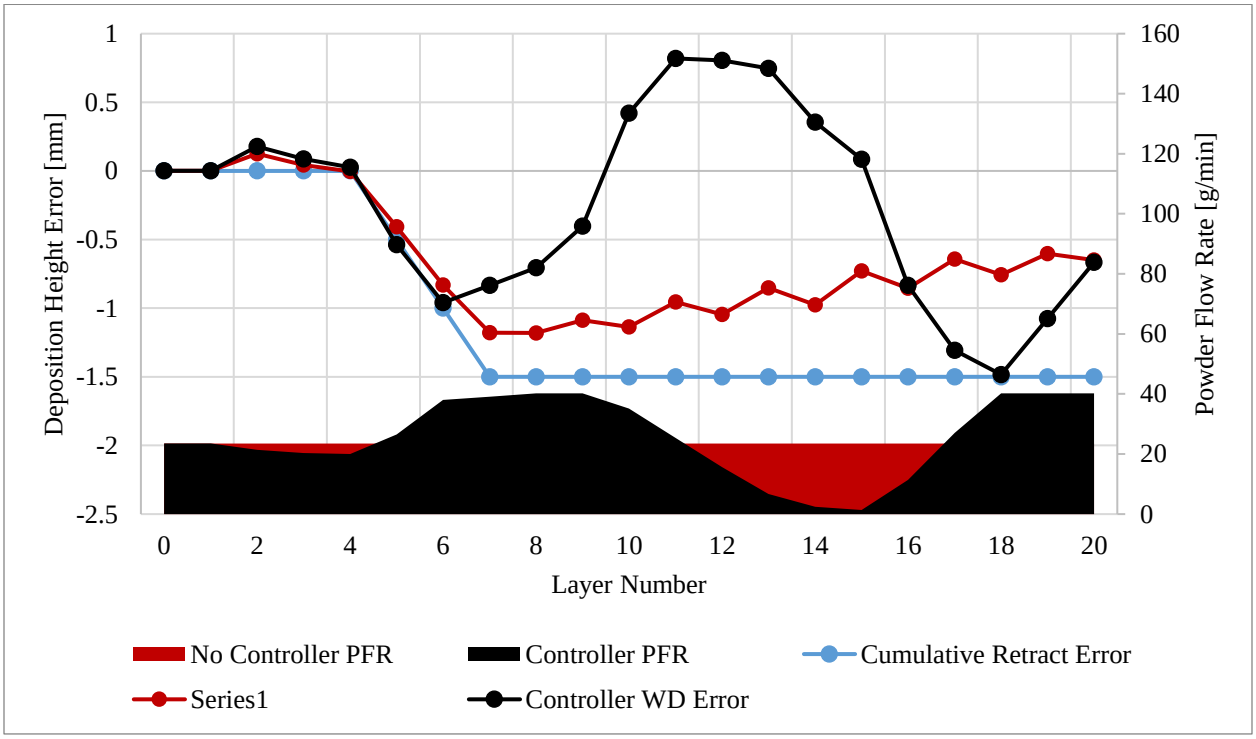

Fig. 4.2: PI Controller 20-Layer Test Data

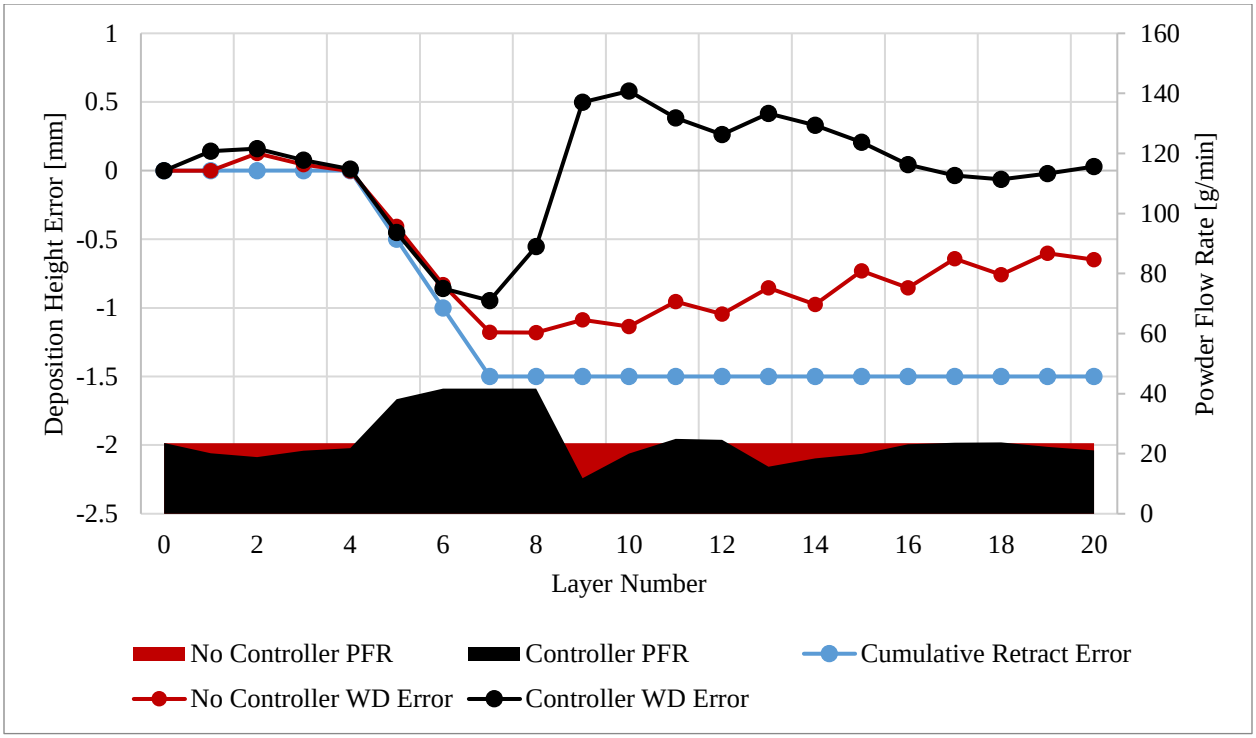

Fig. 4.3: PID Controller 20-Layer Test Data

4.1.3. 120-Layer Thin Wall Deposition with Constant Layer Height

During long builds heat accumulates in the part which causes the clad width to increase while the clad cross-sectional area remains constant, leading to a shorter clad [3]. The flattening of the clads can cause both part underbuilding and severe sloping at the ends of thin wall parts. Heat accumulation can be mitigated by decreasing the laser power as the build progresses and including long interlayer dwelling periods to allow for the heat to diffuse into the part, but both techniques limit DED productivity.

To illustrate the controller's ability to maintain part geometric accuracy over a long deposition without sacrificing DED productivity, 120-layer thin wall parts were built with and without the height controllers. The 99.6 mm tall thin walls were deposited using the deposition parameters in Table 3.1 and initial PFRs of 23.5 g/min. An interlayer dwell of 3 s was used in these longer

depositions to decrease the DED cycle time by 17% compared to a 5 s interlayer dwell. Photos of the two thin wall builds are shown for comparison in Figures 4.6 and 4.7. Figures 4.4 and 4.5 show the height error and PFR during the 120-layer builds for the PI and PID controller.

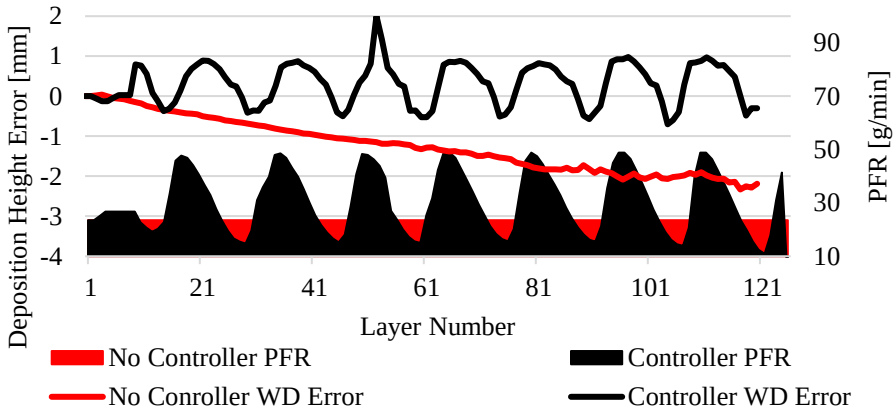

Fig. 4.4: PI Controller observed height error and controller commanded PFR during 120-layer thin wall build.

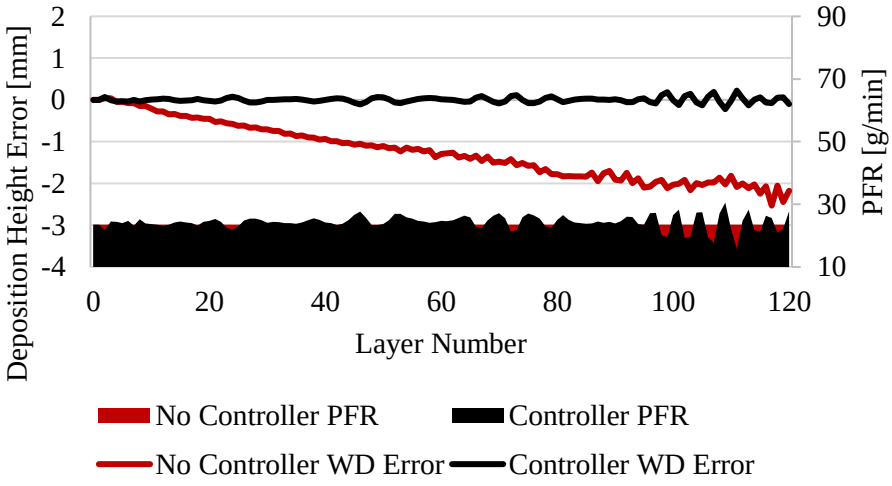

Fig. 4.5: PID Controller observed height error and controller commanded PFR during 120-layer thin wall build.

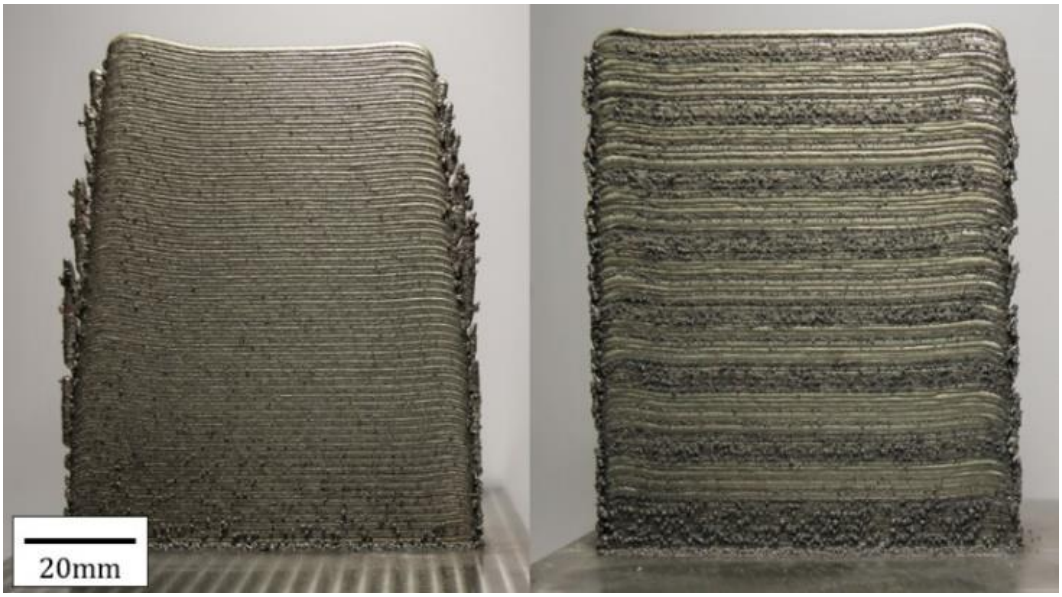

Fig. 4.6: 120-layer thin wall builds with 3 s interlayer dwell (left) without controller and (right) with PI controller

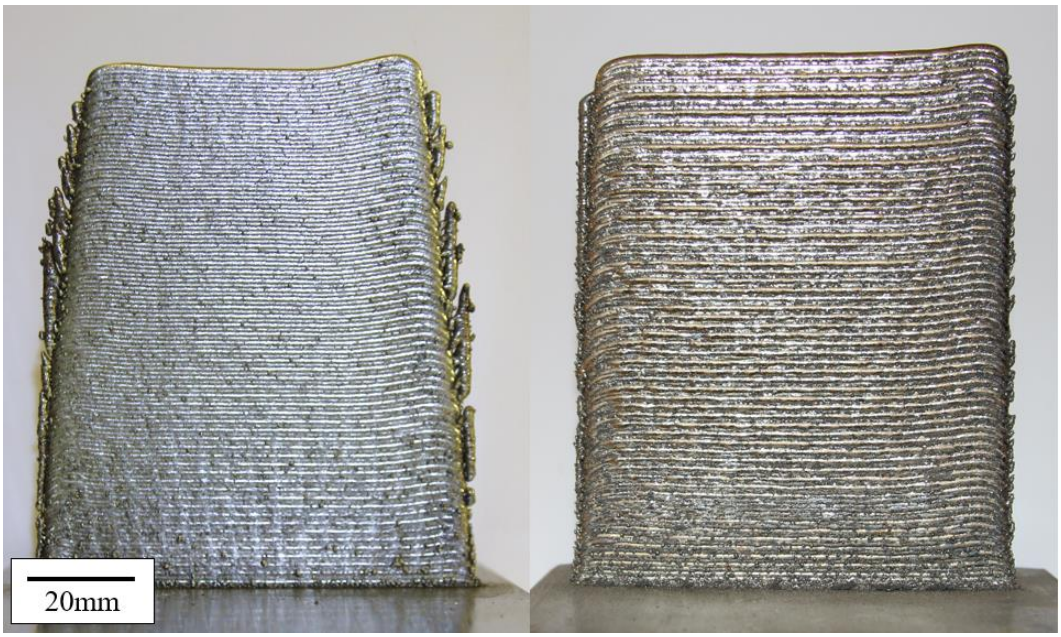

Fig. 4.7: 120-layer thin wall builds with 3 s interlayer dwell (left) without controller and (right) with PID controller

4.1.4. 170-Layer Thin Wall Deposition with Constant Layer Height

Testing with the 120-Layer Thin Wall led to some concern about instability in the PID controller towards the end of the experiment. A 170-Layer thin wall was then performed to assuage any speculation. The results may be viewed in the following figures. A comparison 170-Layer thin wall without the controller was not performed due to an established trend already being viewed in previous experiments.

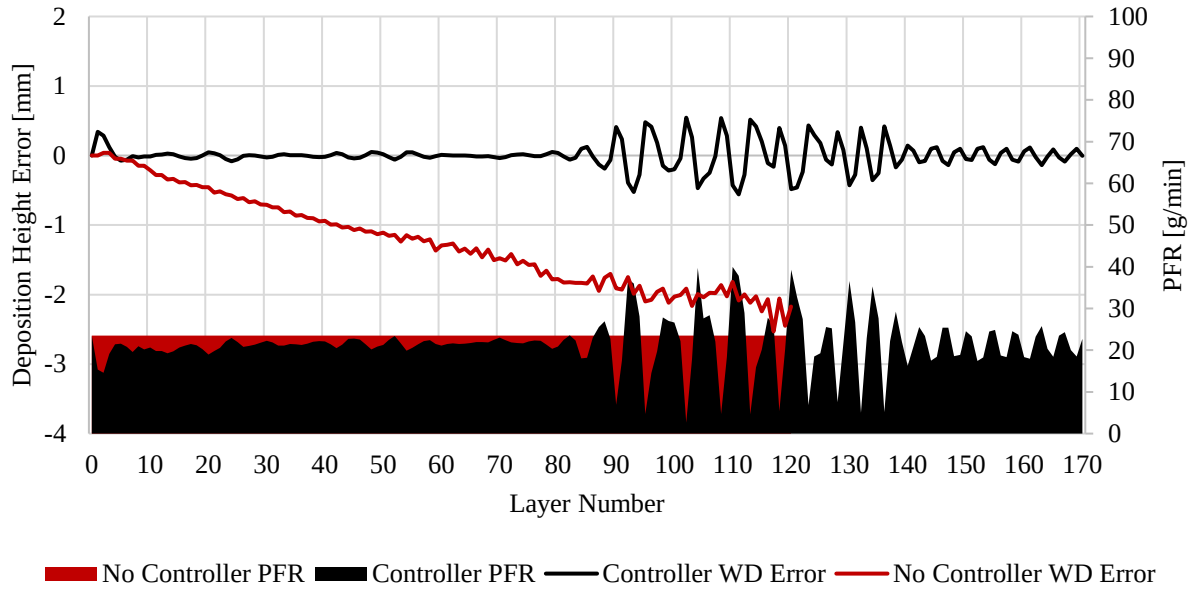

Fig. 4.8: PID Controller observed height error and controller commanded PFR during 170-layer thin wall build.

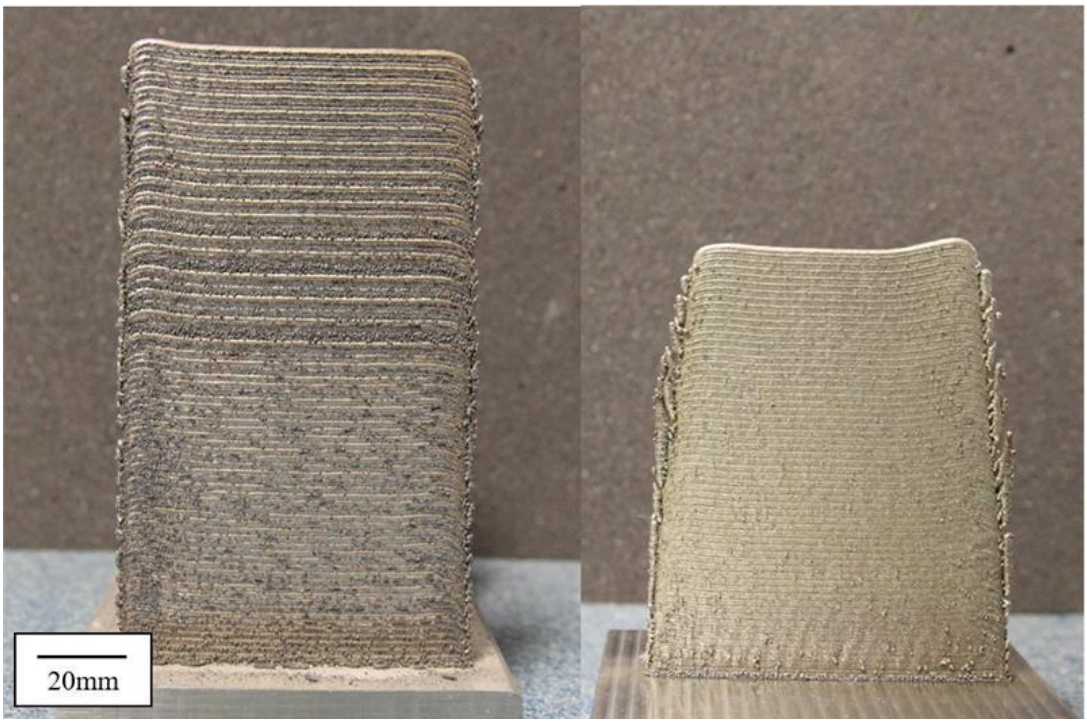

Fig. 4.9: (left) 170-layer thin wall build with 3 s interlayer dwell with PID controller and (right) 120-layer thin wall build with 3 s interlayer without controller

5. DISCUSSION

5.1. Thin Wall Experiments

5.1.1. 10-Layer Thin Wall with Constant Layer Height

Using a control system resulted in a smaller average final height error as can be seen in Figure 4.1 above. A larger variance is observed with the PI and PID controllers, potentially due to the precision in changing the PFR during the deposition process. Nevertheless, the smaller mean part height error and low height variance compared to clad layer height show that the height control system does not adversely affect stable DED processes. The PID controller here displays values centered more closely around 0 mm error which gives some indication that for shorter builds, the PID controller seems to have a more accurate final result than that of the PI controller and without a controller.

5.1.2. 20-Layer Thin Wall with Nonconstant Layer Height

Comparison of the working distance errors between the thin wall build with and without the controller shows how the system detects the working distance error and increases the powder flow to the nozzle. The PFR increase for each controller causes an increase in layer height which eliminates the working distance error considerably. For the case of the PI controller, it is able to make the error positive within 3 layers. The PID controller is able to achieve this within 2 layers after the error is introduced. While the passive height control behavior of the coaxial nozzle can be seen in the height error trend without the controller, the effect is slow. The instability of the PI controller is hinted in these results as there seems to already be oscillatory behavior observed due to the disturbance introduced in these tests, and the final deposition height error is quite close to that achieved without a controller (regular deposition process). However, the PID controller appears to be more robust, stabilizing around zero after overshooting slightly to an overbuild of 0.5mm.

5.1.3. 120-Layer and 170-Layer Thin Wall Depositions with Constant Layer Height

The oscillatory behavior observed in the PI controller is more evident in this deposition. This is what indicated that a more robust controller may be needed to be able to handle the dynamic nature of the DED process. After the PID controller was developed, the oscillations are dampened by 91%. Using PFR modulation to correct for underbuilding due to heat accumulation effects not only maintains the average layer-wise height error near 0, but it also ensures that the edges of the thin wall do not slope excessively as can be seen in the thin wall photos above.

5.2. PI vs PID Control Comparison

While the comparison between the PI and PID control was described above, this is only based on the values from the camera, calculated from the controller. To examine the real measurement against the sensor measurement, a MicroVu Excel HC502 was used to measure the height of the 120-layer thin walls with a camera-based measuring system. The setup can be viewed in Figure 5.1. By exposing light onto the thin wall and having the machine measure the piece given a datum set to the base of the substrate, an excel file listing the height across the top of the thin wall is gathered. A 90% median average, just like what is performed in the control system, is used to remove any outlier points. The values and their comparison can be viewed in Table 5.1. With percent difference values below 1%, the camera sensor measurement system used in this height controller can be deemed to be fairly accurate.

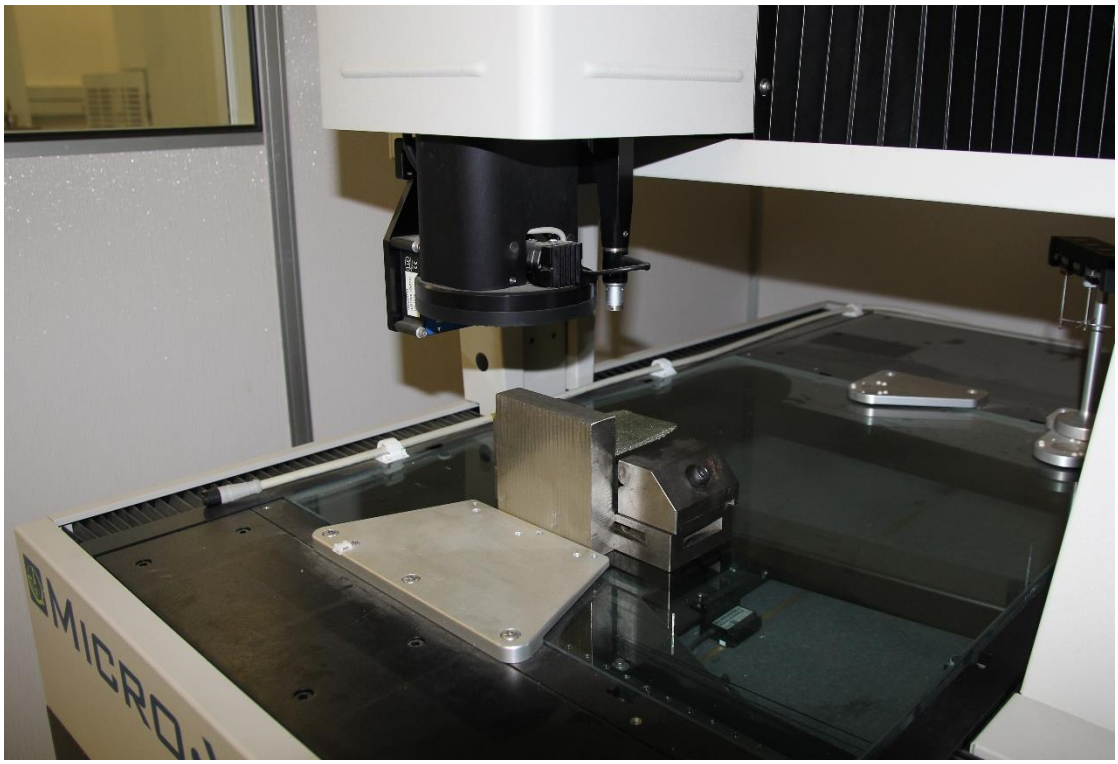

Fig. 5.1: Micro-Vu Camera and Light Measurement Setup

Table 5.1: Final Height Error Sensor, Actual, and Expected Value Comparison

Type	Sensor Value	Actual Value	Percent Difference
No Controller	97.425	97.602	0.18%
PI Controller	99.570	98.637	0.94%
PID Controller	99.503	98.650	0.86%
	Actual Value	**Expected Value**	**Percent Difference**
No Controller	97.602	99.600	2.03%
PI Controller	98.637	99.600	0.97%
PID Controller	98.650	99.600	0.96%

When compared against the actual value, the measurement system developed in this paper can be deemed reasonably precise. However, the actual value of the wall at the end of the deposition should be 99.6mm as it should be 120 layers with 0.83mm thickness per layer. The discrepancy here may also be due to heat accumulation. As the deposition process went on and the heat gathered, the welding lens would get very hot, creating a red tint on the frame. Additionally, the meltpool size would increase due to the clad size increasing as the clads began to flatten and sink on themselves. This all can affect the ability of the camera to garner an accurate top pixel value to measure the clad height from. Ultimately, when the actual value and expected values are compared, the controller developed is able to improve upon the standard system, achieving a relatively accurate final part height. It is able to achieve a less than 1% difference from the expected final value whereas standard procedure led to a 2.03% deviation from the expected final height.

6. CONCLUSIONS AND FUTURE WORK

6.1. Summary

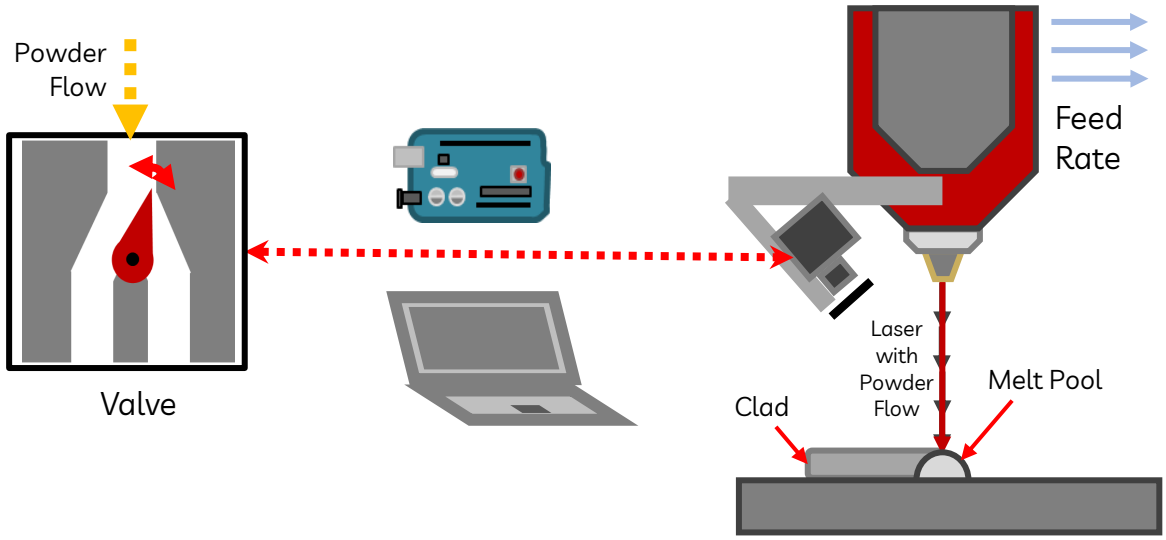

Fig. 6.1: Control System Overview

The in-process clad height control using optical monitoring and rapid PFR modulation via a DPSS was developed and examined. The connections of which are shown in Figure 6.1. A CCD camera is used to measure the meltpool during deposition, and PI and PID controllers calculate a change in PFR to correct deposition errors in the dynamic process that is DED.

To examine the efficacy of each control system developed in order to ascertain the more robust control system, three sets of different thin wall tests were performed. 10-Layer thin wall tests were used to preliminary examine the response of the controllers and how they compare to the DED process to ensure that the controllers do not negatively impact the system. Short, stable builds were produced that showed that both controllers were able to create accurate parts in a short deposition. 20-Layer thin wall builds were used to show the speed in which each controller is able to correct

drastic errors in depositions. While unrealistic within a natural deposition setting, this extreme test case was able to demonstrate how each controller is able to perform under severe disturbances. 120-Layer thin wall tests were performed to demonstrate how the controllers are able to perform against one of the most common issues within the DED process, heat accumulation. While both controllers are able to stabilize the long depositions around 0mm, the PID controller is definitely the better controller in this scenario as it is able to dampen the oscillations viewed in the PI controller results.

This improvement in the DED process stability and productivity can be used to advance the adoption of DED in the industrial manufacturing space for larger parts that require longer build times.

6.2. Future Work

6.2.1. Refinement

There will always be improvements that can be added to the current system. This is the first examination of a system that uses both an optical monitoring system as well as a DPSS. Some limitations found in this setup are the resolution of the camera. By using a camera with more resolution, we may be able to increase the resolution of the pixel-to-mm ratio, which potentially can increase the accuracy of the controller. While the DPSS was able to perform angle position changes in 0.2 increments, if the resolution of this system were expanded, the PFR modulation would be even more accurate. This would require changes to the electrical signaling setup. Heat accumulation in the setup also was a concern as breaks between long depositions were taken to ensure that the parts would not fail due to overheating. By implementing heatsinks into the fixture or onto the camera, this can largely be avoided in the future.

6.2.2. Expand Applications

While thin wall tests were the only type of tests performed in this paper, there can be tests conducted with more complex parts, such as that of a cylinder, block, or even typical industry parts. Due to time limitations, these types of builds were not explored due to the fact that the control program inputs would have to be modified for the various test types. However, by expanding upon the control system programming developed here, there will be an even wider range of applications that can utilize this system.

6.2.3. Increase Complexity

Not only would switching out the components for more expensive, accurate pieces aid in making the system better, but also adding additional sensor components could also aid in the efficiency and accuracy of the system. The drawbacks of this though would be increasing the complexity of the overall system. By implementing a powder flow rate sensor to monitor the PFR during the deposition from the powder splitter, the system would be able to more accurately change the PFR. As the PFR calculation is an estimation based on the calibration process performed prior to deposition, there is no current way to monitor the PFR outputted by the DPSS during the deposition process. By incorporating this sensor, the calibration process would not be needed as the control system would have programming to adjust the angle position based on the true PFR outputted by the DPSS.

A model-based approach was briefly explored as a method for implementing the control system. Unfortunately, there is currently no model for the effect of heat accumulation within the part itself. There is a simplistic linear relationship developed in previous papers, such as [5],

between the clad height and powder flow, but further testing proved that this relationship is dynamic due to the nature of the part once heat is continuously introduced. A model was attempted to be back-calculated from the results of the longer depositions (how clads begin to sink over the deposition), but development seemed too complex at the time. Therefore, a simple experiment-based tuning approach was used instead to build upon the relationship that has been calculated and researched. A model-based design that is more robust and accurate to the conditions of the DED process may be developed in the future to improve upon the system developed in this paper.

Additionally, adding machine learning to have the controller predict the height errors based on deposition type, length, other parameters would increase the accuracy of the system, but also would require several more tests to train the algorithm to perform precisely.

6.3. Conclusion

Two height control systems were developed and tested, and they both were shown to be effective at controlling part geometric accuracy while also allowing for more productive DED parameters to be used over long builds. A comparison of the two control methods showed that the PID control height control system developed is more efficient and accurate in improving upon build discrepancies in the directed energy deposition process. This improvement in the process stability and productivity can be used to advance the adoption of DED in the industrial manufacturing space.

REFERENCES

[1] T. D. Ngo, A. Kashani, G. Imbalzano, K. T. Q. Nguyen and D. Hui, "Additive manufacturing (3D printing): A review of materials, methods, applications and challenges," *Composites Part B: Engineering,* vol. 143, p. 172–196, 6 2018.

[2] R. Liu, Z. Wang, T. Sparks, F. Liou and J. Newkirk, "Aerospace applications of laser additive manufacturing," in *Laser Additive Manufacturing*, Elsevier, 2017, p. 351–371.

[3] J. Dill, M. Soshi and K. Yamazaki, "A study on the effect of directed energy deposition substrate energy on clad geometry," *The International Journal of Advanced Manufacturing Technology,* vol. 109, p. 315–333, 7 2020.

[4] E. Govekar, A. Jeromen, A. Kuznetsov, G. Levy and M. Fujishima, "Study of an annular laser beam based axially-fed powder cladding process," *CIRP Annals,* vol. 67, p. 241–244, 2018.

[5] U. de Oliveira, V. Ocelík and J. T. M. De Hosson, "Analysis of coaxial laser cladding processing conditions," *Surface and Coatings Technology,* vol. 197, p. 127–136, 7 2005.

[6] S. Donadello, M. Motta, A. G. Demir and B. Previtali, "Monitoring of laser metal deposition height by means of coaxial laser triangulation," *Optics and Lasers in Engineering*, vol. 112, p. 136–144, 1 2019.

[7] J. C. Haley, B. Zheng, U. S. Bertoli, A. D. Dupuy, J. M. Schoenung and E. J. Lavernia, "Working distance passive stability in laser directed energy deposition additive manufacturing," *Materials & Design,* vol. 161, p. 86–94, 1 2019.

[8] D. Kono, H. Yamaguchi, Y. Oda and T. Sakai, "Stabilization of standoff distance by efficient and adaptive updating of layer height command in directed energy deposition," *CIRP Journal of Manufacturing Science and Technology*, vol. 31, p. 244–250, 11 2020.

[9] I. Garmendia, J. Pujana, A. Lamikiz, M. Madarieta and J. Leunda, "Structured light-based height control for laser metal deposition," *Journal of Manufacturing Processes,* vol. 42, p. 20–27, 6 2019.

[10] I. Garmendia, J. Leunda, J. Pujana and A. Lamikiz, "In-process height control during laser metal deposition based on structured light 3D scanning," *Procedia CIRP,* vol. 68, p. 375–380, 2018.

[11] L. Tang and R. G. Landers, "Layer-to-Layer Height Control for Laser Metal Deposition Process," *Journal of Manufacturing Science and Engineering,* vol. 133, p. 021009, 4 2011.

[12] S. Takushima, D. Morita, N. Shinohara, H. Kawano, Y. Mizutani and Y. Takaya, "Optical in-process height measurement system for process control of laser metal-wire deposition," *Precision Engineering,* vol. 62, p. 23–29, 3 2020.

[13] M. Zeinali and A. Khajepour, "Height Control in Laser Cladding Using Adaptive Sliding Mode Technique: Theory and Experiment," *Journal of Manufacturing Science and Engineering,* vol. 132, p. 041016, 8 2010.

[14] L. Song, V. Bagavath-Singh, B. Dutta and J. Mazumder, "Control of melt pool temperature and deposition height during direct metal deposition process," *The International Journal of Advanced Manufacturing Technology,* vol. 58, p. 247–256, 1 2012.

[15] S. Liu and R. Kovacevic, "Statistical analysis and optimization of processing parameters in high-power direct diode laser cladding," *The International Journal of Advanced Manufacturing Technology*, vol. 74, p. 867–878, 9 2014.

[16] M. Soshi, C. Yau and R. Kusama, "Development and evaluation of a dynamic powder splitting system for the directed energy deposition (DED) process," *CIRP Annals*, vol. 69, p. 341–344, 2020.

[17] T. N. Mundhenk, M. J. Rivett, X. Liao and E. L. Hall, "Techniques for fisheye lens calibration using a minimal number of measurements," Boston, 2000.

[18] Kiam Heong Ang and Chong, G. and Yun Li, "PID control system analysis, design, and technology," *IEEE Transactions on Control Systems Technology*, vol. 13, p. 559–576, 7 2005.

[19] J. Zhong, "PID Controller Tuning: A Short Tutorial," p. 13.

[20] B. R. Copeland, "The Design of PID Controllers using Ziegler Nichols Tuning," p. 4.

APPENDICES

A: BOM and Working Drawings of Mechanical Fixture for Camera System

The following pages include the various drawings for the fixturing system developed to attach a camera sensor to the LT65 3D for research purposes.

ITEM NO.	DESCRIPTION	QTY.
1	Filter Holder	1
2	Frame Base	1
3	Frame Cover	1
4	ELP Camera	1
5	Corner Bracket, 1-1/2" x 1-1/2" x 1/2"	2
6	Lasertec 65 3D Hybrid Mounting Plate	1
7	Sheet Metal Attachment Plate	1
8	Adjustment Rod	1
9	Socket Head Cap Screw, M5x70L	1
10	Socket Head Cap Screw M5x35L	2

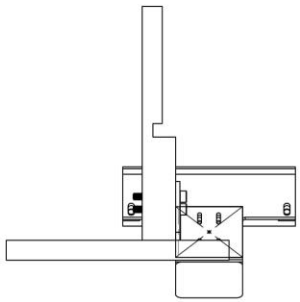

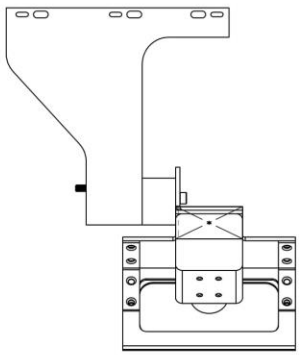

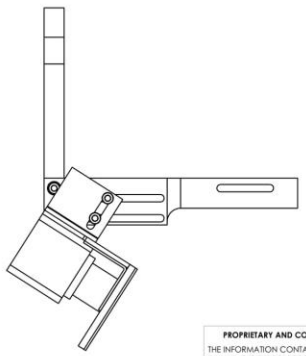

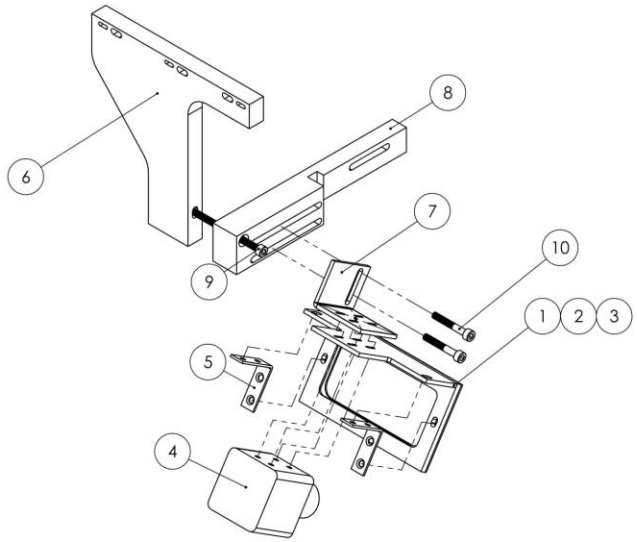

		UNLESS OTHERWISE SPECIFIED:		NAME	DATE
		DIMENSIONS ARE IN INCHES TOLERANCES: FRACTIONAL ± ANGULAR: MACH ± BEND ± TWO PLACE DECIMAL ± THREE PLACE DECIMAL ±	DRAWN	V. ZHOU	
			CHECKED	V. ZHOU	
			ENG APPR.		
			MFG APPR.		
		INTERPRET GEOMETRIC TOLERANCING PER:	Q.A.		
		MATERIAL	COMMENTS:		
NEXT ASSY	USED ON	FINISH			
APPLICATION		DO NOT SCALE DRAWING			

ARMS LAB

TITLE:

CAMERA SENSOR ATTACHMENT ASSY

SIZE	DWG. NO.	REV
B		
SCALE: 1:3	WEIGHT:	SHEET 1 OF 1

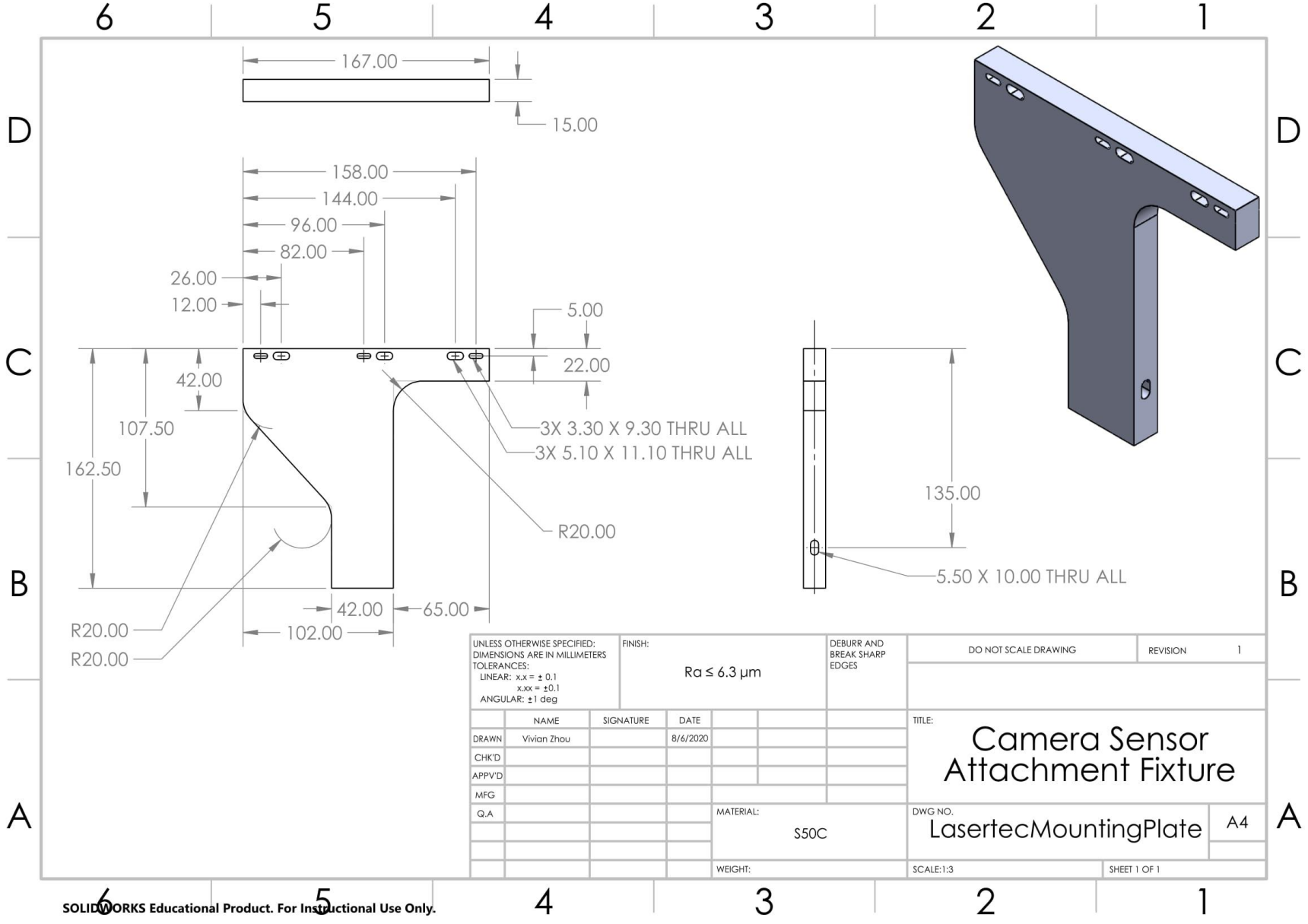

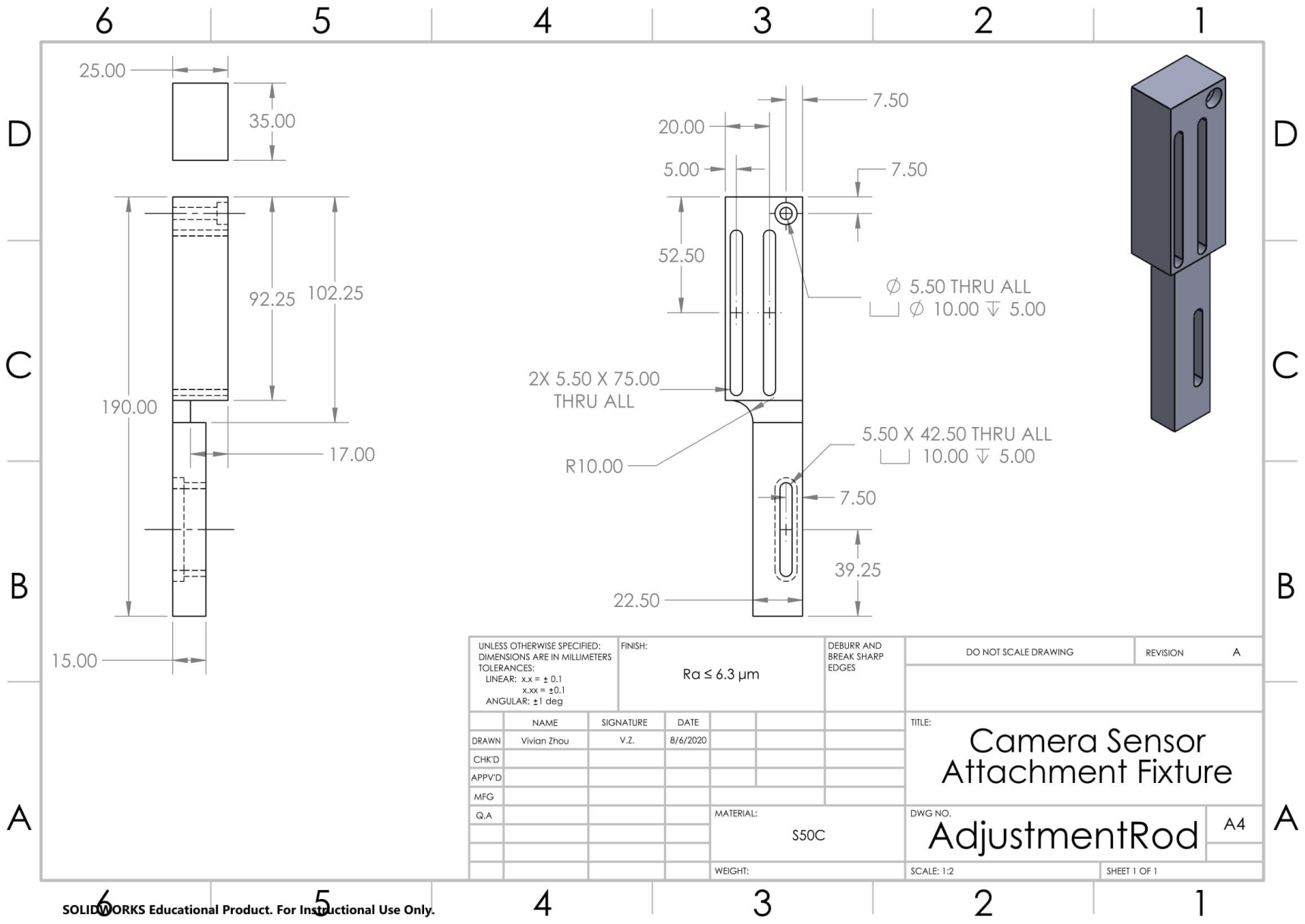

Mfg. Notes: Use 11 Gauge S50C Sheet Metal. Minimum bending radius of 0.5mm.

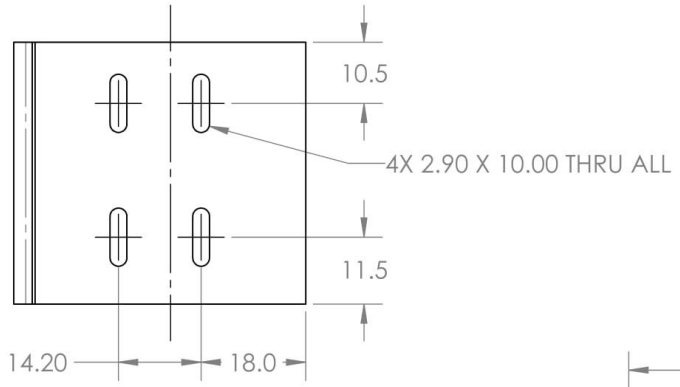

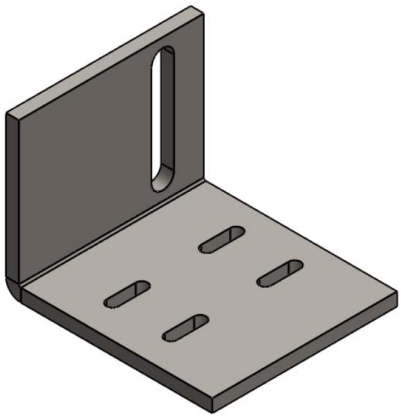

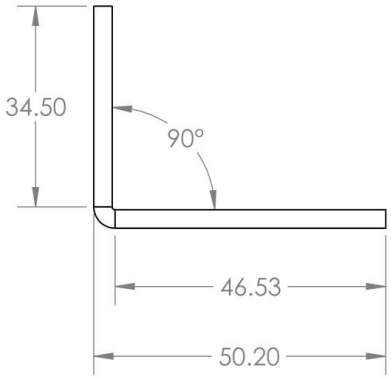

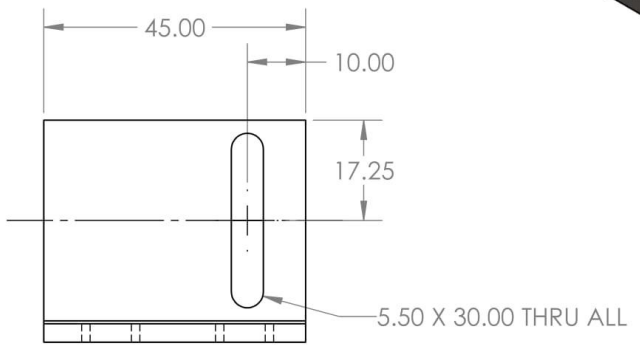

UNLESS OTHERWISE SPECIFIED: DIMENSIONS ARE IN MILLIMETERS TOLERANCES: LINEAR: x.x = ± 0.1, x.xx = ±0.1 ANGULAR: ± 1 deg		FINISH: Regular Sheet Metal Finish		DEBURR AND BREAK SHARP EDGES		DO NOT SCALE DRAWING	REVISION
	NAME	SIGNATURE	DATE			TITLE: Camera Sensor Attachment Fixture	
DRAWN	Vivian Zhou		8/7/2020				
CHK'D							
APPV'D							
MFG							
Q.A				MATERIAL: S50C		DWG NO. AttachPlate_Sheet	A4
				WEIGHT:		SCALE:1:1	SHEET 1 OF 1

Mfg. Notes: Use 11 Gauge S50C Steel Sheet Metal.

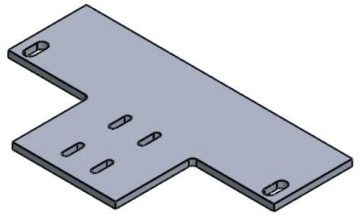

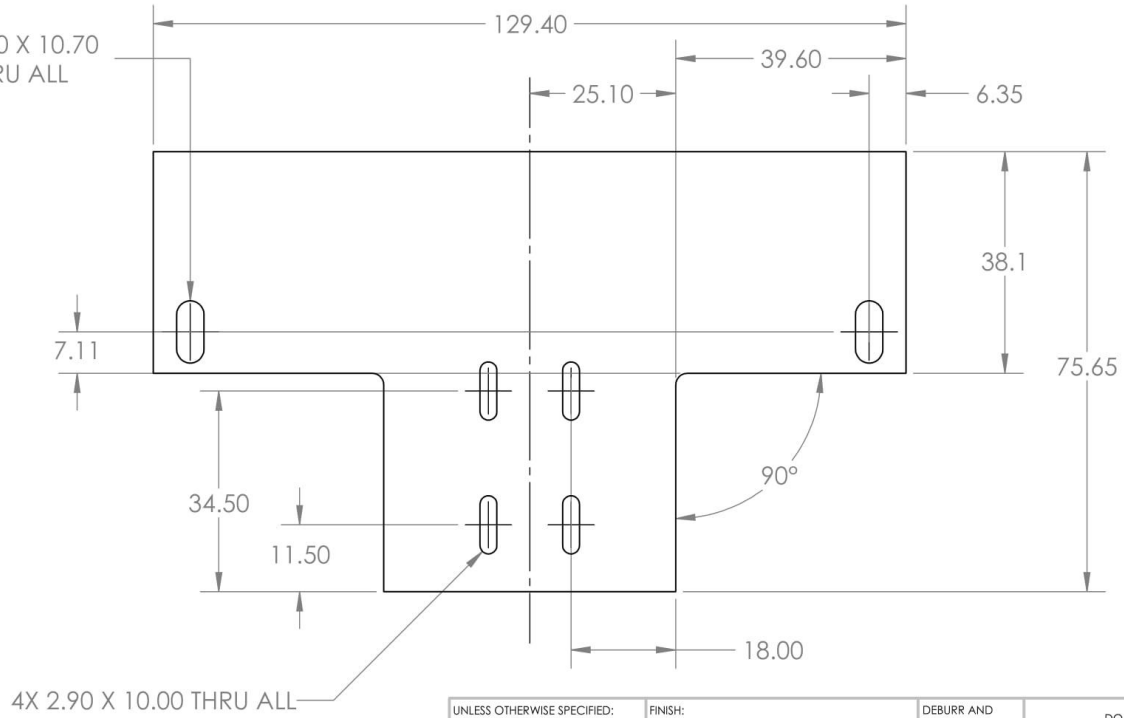

UNLESS OTHERWISE SPECIFIED: DIMENSIONS ARE IN MILLIMETERS TOLERANCES: LINEAR: x.x = ± 0.1 x.xx = ±0.1 ANGULAR: ± 1 deg	FINISH: Regular Sheet Metal Finish					DEBURR AND BREAK SHARP EDGES	DO NOT SCALE DRAWING / REVISION
	NAME	SIGNATURE	DATE				TITLE: Camera Sensor Attachment Fixture
DRAWN	Vivian Zhou		8/5/2020				
CHK'D							
APPV'D							
MFG							
Q.A				MATERIAL: S50C			DWG NO. Camera Filter Attachment / A4
				WEIGHT:		SCALE:1:1	SHEET 1 OF 1

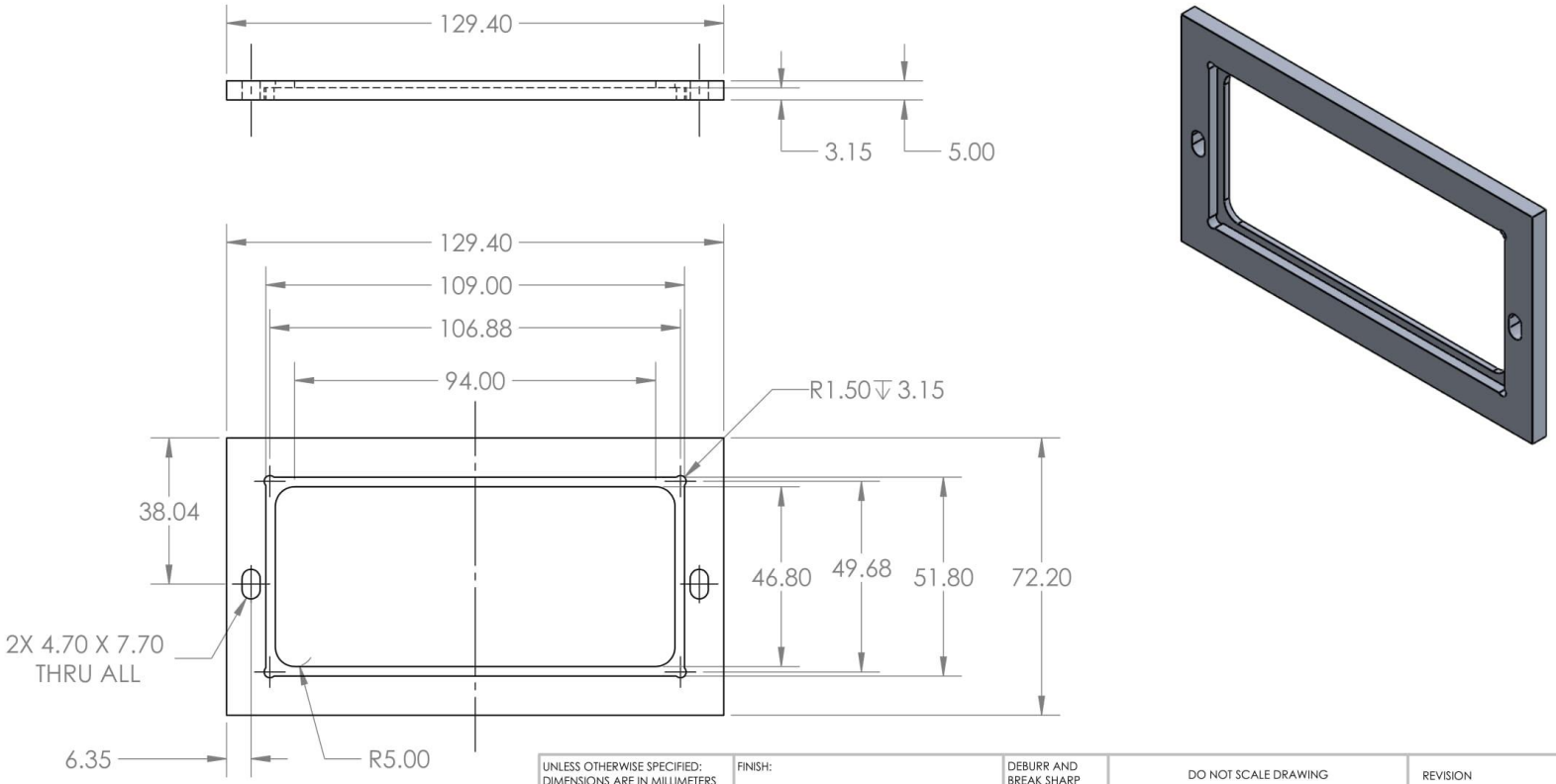

UNLESS OTHERWISE SPECIFIED: DIMENSIONS ARE IN MILLIMETERS TOLERANCES: LINEAR: x.x = ± 0.1, x.xx = ±0.1 ANGULAR: ± 1 deg	FINISH: Ra ≤ 6.3 µm		DEBURR AND BREAK SHARP EDGES			DO NOT SCALE DRAWING	REVISION
	NAME	SIGNATURE	DATE			TITLE: Camera Sensor Attachment Fixture	
DRAWN	Vivian Zhou		8/6/2020				
CHK'D							
APPV'D							
MFG							
Q.A				MATERIAL: S50C		DWG NO. FrameBase	A4
				WEIGHT:		SCALE:1:1.5	SHEET 1 OF 1

Mfg. Notes: Use 16 Gauge S50C Sheet Metal.

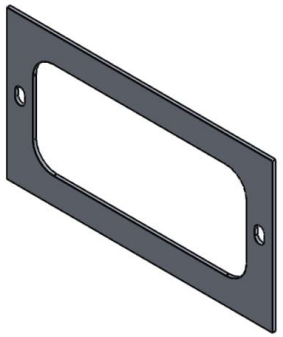

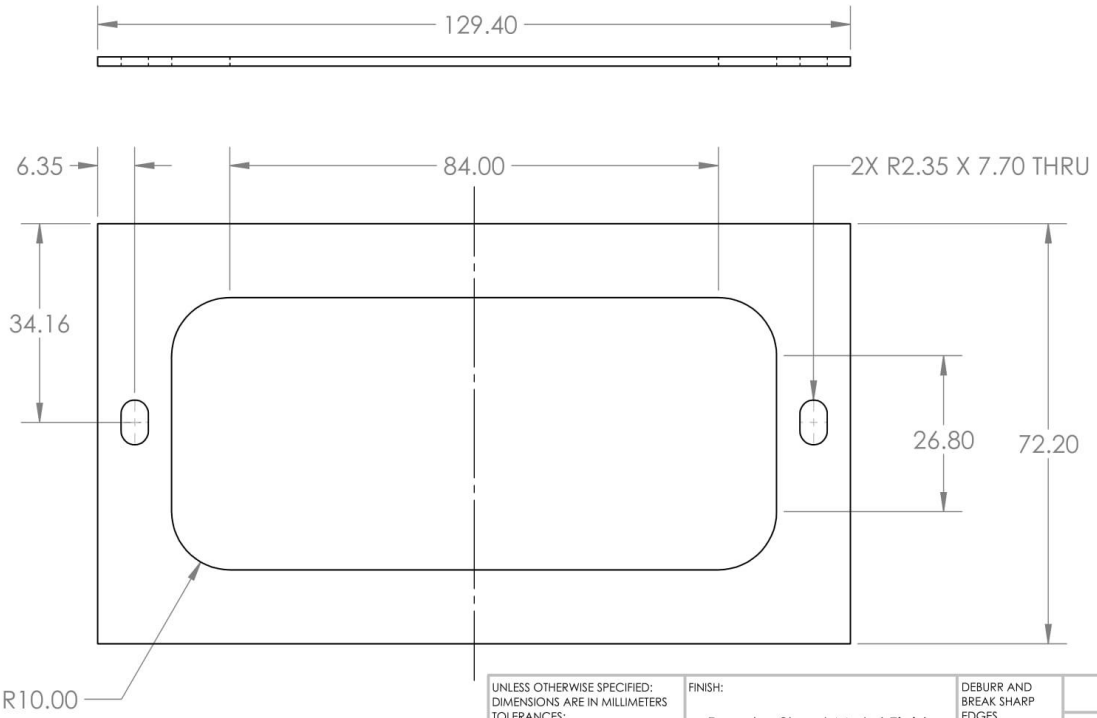

UNLESS OTHERWISE SPECIFIED: DIMENSIONS ARE IN MILLIMETERS TOLERANCES: LINEAR: x.x = ± 0.1, x.xx = ±0.1 ANGULAR: ± 1 deg	FINISH: Regular Sheet Metal Finish		DEBURR AND BREAK SHARP EDGES			DO NOT SCALE DRAWING	REVISION
	NAME	SIGNATURE	DATE			TITLE: Camera Sensor Attachment Fixture	
DRAWN	Vivian Zhou		8/6/2020				
CHK'D							
APPV'D							
MFG							
Q.A				MATERIAL: S50C		DWG NO. FrameCover	A4
				WEIGHT:		SCALE:1:1	SHEET 1 OF 1

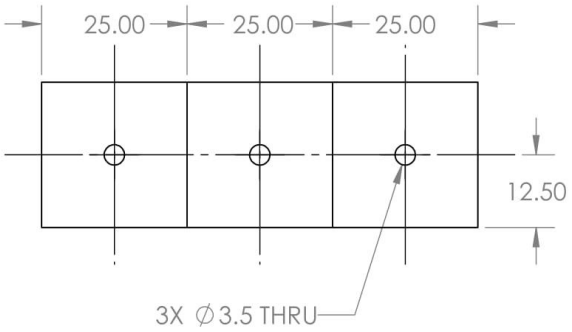

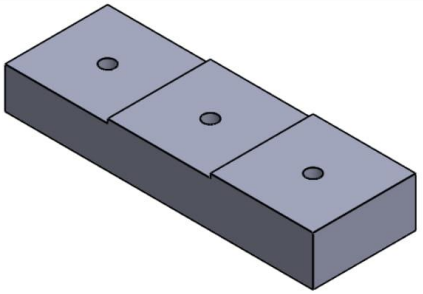

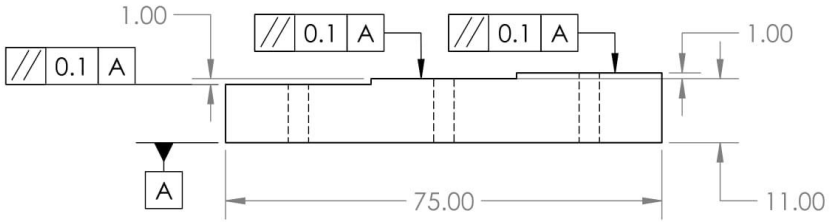

UNLESS OTHERWISE SPECIFIED: DIMENSIONS ARE IN MILLIMETERS TOLERANCES: LINEAR: x.x = ± 0.1, x.xx = ±0.1 ANGULAR: ± 1 deg	FINISH: Ra ≤ 3.2 µm		DEBURR AND BREAK SHARP EDGES			DO NOT SCALE DRAWING	REVISION
	NAME	SIGNATURE	DATE			TITLE: Stepper Block	
DRAWN	Vivian Zhou		8/5/2020				
CHK'D							
APPV'D							
MFG							
Q.A				MATERIAL: S50C		DWG NO. Stepper Block	A4
				WEIGHT:		SCALE:1:1	SHEET 1 OF 1

B: Key Python Code for Image Analysis and Control System Architecture

The following are code exports of main sections of the Python code used to create the control system. Other files that concern defining variables, creating the GUI, and exporting the data are not included.

File - C:\Users\VZ\Downloads\PFRControlSysCamera - Averaging-selected\main_func.py

```
 1 import time
 2
 3 import cv2
 4 from PIL import Image, ImageTk
 5
 6 import capture_start
 7 import convert_mm
 8 import count_layer
 9 import define_variable
10 import draw
11 import extract_target
12 import gui_design
13 import obtain_target_info
14 import output
15 import controller_calcs
16 import write_arduino
17 import numpy as np
18 from scipy import stats
19
20 global cap
21
22
23 def func():
24     global img, img2
25     ret, frame = capture_start.cap.read()
26     frame = cv2.resize(frame, (1280, 720))
27
28     clean_vid = frame.copy()
29     binary = extract_target.func(frame)
30     binary_display = cv2.resize(binary, (256, 144))
31
32     try:
33         x_min, top, cols, rows, area, height_px, centroid = obtain_target_info.func(binary)
34         define_variable.no_obj = 0
35         count_layer.laser_on()
36
37     except ValueError:
38         x_min = top = cols = rows = area = height_px = centroid = 0
39         cv2.putText(frame, "Object not found", (65, 590), cv2.FONT_HERSHEY_TRIPLEX, 1, (0, 0, 255), 2)
40         define_variable.no_obj = 1
41         count_layer.laser_off()
42
43     # convert height of the laser spot TOP in pixel to mm
44     top_mm = convert_mm.func(top)
45     height_mm = convert_mm.func(height_px)
46
47     elapsed_time = time.time() - define_variable.start
48
49     frame = draw.func(frame, cols, rows, x_min, top, centroid, int(height_px), height_mm, top_mm,
50                       define_variable.layer)
51
52     if define_variable.record_flag == 1:
53
54         output.func(frame, elapsed_time, top_mm, rows, top, str(round(height_px, 8)), height_mm, clean_vid)
55     if define_variable.layer != 0:  # if layer after first layer (scanning layer)
56         if (define_variable.laser == 0) and ((len(define_variable.error_list)) > 5) and \
57                 (define_variable.ard == 0):
58             # in between deposition layers, calc 90% middle average
59             define_variable.avg_error = stats.trim_mean(define_variable.error_list, 0.05)  # 5% off both
   ends [px]
60             define_variable.error_bilayer_list.append(define_variable.avg_error)  # [px]
61             define_variable.error_list.clear()  # clear error list after appending average to layer list
62             if define_variable.dep == 0:
63                 # if the error is above a certain threshold, immediately send a signal to the arduino
64                 define_variable.avg_error_2_mm = convert_mm.func(define_variable.avg_error) -
   define_variable.retract
65                 # set the bilayer list to the single large error
66                 define_variable.error_bilayer_list = [define_variable.avg_error]  # [px]
```

```
                define_variable.a = 1
            if (len(define_variable.error_bilayer_list) > 1) and (define_variable.layer != 1):
                # after 2 layers recorded, average the prev two layers and send to arduino
                # calc error and convert to mm
                define_variable.avg_error_2 = np.mean(define_variable.error_bilayer_list)  # [px]
                define_variable.avg_error_2_mm = convert_mm.func(define_variable.avg_error_2)
                define_variable.avg_error_2_mm = define_variable.avg_error_2_mm - define_variable.retract
                define_variable.a = 1
            if define_variable.a:
                # convert mm to pt pos to send to arduino
                define_variable.new_pfr, define_variable.degree, define_variable.deg_target,
   define_variable.pt = \
                    controller_calcs.func(define_variable.avg_error_2_mm)
                define_variable.avg_error_prev = define_variable.avg_error_2_mm  # save pre error
                define_variable.pfr = define_variable.new_pfr  # UPDATE PFR
                # send to arduino
                if gui_design.ctrl_check.get() == 1:  # if we want controller to be active
                    write_arduino.func(define_variable.pt)  # send to arduino
                else:  # else, do nothing but raise flag that we "sent" data to arduino
                    print("Sending to Arduino...")
                    define_variable.ard = 1  # do not send to arduino again during this dwell time
                if len(define_variable.error_bilayer_list) > 1:  # if there were prev 2 layer averages
                    define_variable.error_bilayer_list.pop(0)  # remove first value
                define_variable.a = 0
        elif (define_variable.no_obj == 0) and (define_variable.laser == 1):
            define_variable.error = top
            define_variable.error_list.append(define_variable.error)
            define_variable.ard = 0

    if ret:
        img_resize = cv2.resize(frame, (640, 360))
        img = ImageTk.PhotoImage(Image.fromarray(cv2.cvtColor(img_resize, cv2.COLOR_BGR2RGB)))
        gui_design.canvas_main.create_image(320 + 10, 180 + 15, image=img)
        img2 = ImageTk.PhotoImage(Image.fromarray(cv2.cvtColor(binary_display, cv2.COLOR_BGR2RGB)))
        gui_design.canvas_binary.create_image(128, 72, image=img2)
    else:
        print("u-Fail")

    gui_design.tree.delete(*gui_design.tree.get_children())
    gui_design.tree.insert("", index="end", values=("T-C Diff [px]", str(round(height_px - top, 4))))
    gui_design.tree.insert("", index="end", values=("Height [mm]", str(round(top_mm, 4))))
    gui_design.tree.insert("", index="end", values=("Layer", str(define_variable.layer)))
    gui_design.tree.insert("", index="end", values=("New PFR", str(round(define_variable.new_pfr, 4))))
    gui_design.tree.insert("", index="end", values=("Degree", str(define_variable.deg_target)))
    gui_design.tree.insert("", index="end", values=("Error Layers", str(define_variable.num_error_layers)))
    gui_design.tree.insert("", index="end", values=("Error Amount", str(define_variable.error_amt)))

    gui_design.root.after(1, func)

```

File - C:\Users\VZ\Downloads\PFRControlSysCamera - Averaging-selected\obtain_target_info.py

```python
import cv2
import numpy as np


def func(mask):
    # labeling
    label = cv2.connectedComponentsWithStats(mask)
    # get blob data
    data = np.delete(label[2], 0, 0)
    # get list of area size
    moment = data[:, 4]
    # get index of largest area
    index = np.argmax(moment)
    # left
    x_min = data[index, 0]
    # top
    y_min = data[index, 1]
    # left to right
    length_lr = data[index, 2]
    # top to bottom
    length_tb = data[index, 3]
    # area size
    area = data[index, 4]
    # get list of centroid coordinates
    centroid_list = np.delete(label[3], 0, 0)
    # get centroid coordinates of largest area
    centroid = centroid_list[index]
    # get y-coordinate of largest area (= height)
    object_height = (centroid[1])

    return x_min, y_min, length_lr, length_tb, area, object_height, centroid

```

File - C:\Users\VZ\Downloads\PFRControlSysCamera - Averaging-selected\controller_calcs.py

```python
import define_variable
import numpy as np


def func(e):
    # derivative term
    d_error = e - define_variable.avg_error_prev  # change in error
    der_term = define_variable.F * define_variable.d * (-1) * d_error * define_variable.Kd  # derivative term
    if define_variable.layer < 3:  # if first, second layers, perform PI control (no change in error)
        der_term = 0
    # integral term
    define_variable.e_list.append(e)
    int_term = define_variable.F * define_variable.d * (-1) * sum(define_variable.e_list) * define_variable.Ki

    # PID CONTROLLER ####
    new_pfr = (23.5 + int_term) + der_term + (define_variable.F * define_variable.d * (-1.0 * e) * define_variable.Kp)
    # + prop term

    # EQUATION BASED ON CURVE FIT
    if new_pfr > define_variable.pfr_0 * define_variable.A:
        new_pfr = define_variable.pfr_0 * define_variable.A
    elif new_pfr <= 0:
        new_pfr = 0.01

    degree = (np.log(new_pfr / (define_variable.pfr_0 * define_variable.A)) / (-1 * define_variable.k)) ** (
            1 / define_variable.n)

    if degree >= 22:
        degree = 22
    elif degree <= 0:
        degree = 0
    define_variable.last_deg = degree
    deg_target = getNearestElement(define_variable.deg, degree)
    pt = int(5 * deg_target)
    return new_pfr, degree, deg_target, pt


def getNearestElement(array, value):
    array = np.asarray(array)
    idx = (np.abs(array - value)).argmin()
    return array[idx]

```

File - C:\Users\VZ\Downloads\PFRControlSysCamera - Averaging-selected\write_arduino.py

```
 1 import define_variable
 2 import time
 3 import serial
 4 from serial import Serial
 5
 6
 7 def func(pt):
 8     define_variable.ard = 1
 9     define_variable.arduino.write(str(pt).encode())
10     time.sleep(0.55)
11
```